1   AUTHORS' RESPONSE TO REFEREE #1

2   **Research article:**

3   Comparing an insurer's perspective on building damages with modelled damages from pan-European

4   winter windstorm event sets: a case study from Zurich, Switzerland (Nat. Hazards Earth Syst. Sci.

5   Discuss., https://doi.org/10.5194/nhess-2020-115, in review; submitted on 07 April 2020)

6   **Authors:**

7   Christoph Welker, Thomas Röösli, David N. Bresch

8   *We thank the referee Dr. Alexandros Georgiadis for his final comments, which have further improved the*

9   *quality of the paper.*

10   *The original comments from the referee are listed below directly followed by our responses in blue and*

11   *italic and changes to the manuscript in blue and bold.*

12   Firstly, I want to thank the authors of the paper for their detailed and robust responses. I am very happy

13   the authors payed a lot of attention to provide persuasive answers to all four research questions in my

14   original review. Particular attention is given to respond to question (2), which was substantiated with an

15   additional piece of analysis (regarding the uncertainty calculation) that I think will make a good addition

16   to the paper.

17   Summaries of two (out of the four) main questions discussed in the review are listed below, along with

18   the author's answers […], followed with my final comment/view […].

19   <u>Review point</u>: The proposed approach to produce a probabilistic event set by perturbing/expanding the

20   WISC historical events is technically correct and appropriate given the scope of the analysis. Having said

21   that, although acceptable, the approach is not novel. [...] the main catastrophe model vendors in the

22   market (RMS, AIR, AON Impact forecasting and more) tend to provide probabilistic windstorm solutions

23   based on outputs extracted from a variety of long global climate model (GCM) runs, calibrated (often

24   fitted) against the available historical record. The advantage of this approach is that the simulation

25   generates physically realistic storms that are not constrained by the attributes/parameters of the seeding

26   historical windstorms.

27   <u>Author's response</u>: As the referee rightly states, there are many different ways to assess the risks from

28   European winter windstorms. We show two possible approaches in this paper [...] The paper was not

29   necessarily about showing a new methodology. In our view, the recent development of freely accessible

30   data on windstorm footprints (WISC) in combination with an open source damage model (CLIMADA)

31   opens up new opportunities for applied research and provides a straightforward entry point for insurance

32   companies to model the risks associated with winter windstorms in Europe – thus providing an additional

33   / alternative perspective compared to inhouse or commercial models (as listed by the referee above). The

34   application example we give is something new because of the open source concept presented.

35   Reviewer's response: I understand and agree with the paper aim. You are not looking for a novel

36   modelling methodology, instead, you provide an application example of how to extend the information

37   available in the available WISC data and build an inhouse model. I think there is merit in your approach.

38   *Thanks for the positive comment!*

39   The approach to expand the WISC historical events and determine the frequencies of the offspring

40   probabilistic storms (GEV distribution fitted to the historical SSI values) has merit, and the concluding

41   results in paragraphs 3.2 and 3.3, also provided in table 2, are realistic. [...] I understand why the authors

42   prefer to retain the confidence interval based on the WISC historical set (CHF 19M to 33,000M), yet this

43   reduces somewhat the functionality of the probabilistic expansion model. It's main objective is to provide

44   a tail view. Here are a few suggestions: (a) Sample randomly the equivalent of 250 or 500 years of storms

45   and build multiple exceedance frequency curves for each sample. (b) Estimate multiple probabilistic

46   extensions of the WISC historic event set with different initial assumptions … (c) combination of the

47   above two ideas.

48   Author's response: We thank the referee for his suggestions. We have implemented all of them and

49   discuss the results in the following. As a conclusion, we would still argue, that the yellow ribbon in Fig. 2

50   (i.e., the sampling uncertainty of the modelled damages based on "WISC 168 historic") is the best

51   illustration of the uncertainty for "WISC probabilistic extension". We will include this argumentation in

52   the manuscript, alongside the arguments already provided in this response. [...] We are aware that the

53   parameter uncertainty regarding the event set "WISC probabilistic extension" is important, especially in

54   comparison with "WISC historic". However, in our opinion this source of uncertainty is not fully

55   estimated and sufficiently illustrated with 184 such a resampling methodology. [...] We resampled (choice

56   with replacement) the historic events [...] Then we created a probabilistic event set for each of these

57   samples. The 90-% confidence interval is again given by the 5th and 95th percentiles of all samples. This is

58   the best possible way we achieved to illustrate at least part of the uncertainty that originates from the fact

59   that the best-estimate of the distribution of the pan-European Storm Severity Index is unknown and thusly

60   the parameters for the creation of the probabilistic sets can only be chosen with a certain degree of

61   uncertainty. The uncertainty estimation up until a 30-year return period follows approximately the

62   uncertainty estimation for "WISC historic"; at higher return periods the uncertainty estimation is levelling

63   off, probably due to the limited ability of our probabilistic approach to create very different (e.g., much

64 stronger) events from the seeding historic set. Therefore, we argue that the shown difference between the

65 yellow ribbon and the red ribbon could be misleading. [...] The results for the referee's suggestion 2c,

66 which is a combination of his suggestions 2a and 2b, are given in Fig. R1-3. [...] Whereas this

67 combination provides a smooth illustration of the resampling uncertainty, it still suffers from the same

68 problem as the illustration in Fig. R1-2. Therefore, we would still argue that the yellow ribbon in Fig. 2 is

69 the best illustration of the uncertainty for "WISC probabilistic extension".

70 Reviewer's response: Thanks for the extensive work that resulted in the uncertainty estimations given by

71 the red ribbons in Fig R1-1 to 3. I think that this analysis illustrates very clearly three different levels of

72 uncertainty estimations, blue, yellow and red ribbons. I should clarify that I do agree with your

73 conclusion, the yellow ribbon gives the best account of the uncertainties associated with the "WISC

74 probabilistic extension" and it should be included in the paper. This does not change my view though that

75 the 'reduced' uncertainty in the red ribbon from the resampling approach also has merit and it should be

76 included in the paper as well, not to replace the (yellow ribbon) full WISC probabilistic extension

77 uncertainty, but to complement it. Yes, the uncertainty estimation from resampling is 'incomplete' yet it

78 can be helpful in the practical case of model. The Uncertainty in the yellow ribbon is too broad to provide

79 a comparison criterion between two different exceedance frequency curves from different models, (e.g.

80 WISC hazard + GVZ versus WISC hazard + CLIMADA) Thus, I think inclusion of the resampling

81 uncertainty (red ribbon) in addition to the full WISC probabilistic extension uncertainty) yellow ribbon

82 can be advantageous for your paper.

83 *The referee is right to point out the advantage of the red ribbon, illustrating the range of the*

84 *bootstrapped damage frequency curves of the modelled damages based on "WISC probabilistic*

85 *extension". Therefore, we would like to include the referee's suggestion in the revised*

86 *manuscript, specifically the importance of the tail view of probabilistic datasets and the*

87 *comparison of different damage models for certain applications in the insurance industry. In*

88 *order to show the uncertainty range of the individual damage datasets, we use the following*

89 *ribbons in Fig. 2 of the paper:*

90 *1. Blue ribbon: sampling uncertainty of insured damages*

91 *2. Yellow ribbon: sampling uncertainty of modelled damages based on "WISC historic"*

92 *3. Red ribbon: probabilistic envelope of the modelled damages based on "WISC probabilistic*

93 *extension"*

94 *Please note that the red ribbon with "probabilistic envelope" is labelled differently than the other*

95 *two ribbons (i.e., sampling uncertainty), which is to emphasise that the red ribbon was derived*

96 *differently than the other two.*

Specifically, we would make the following additions to the sections Data and methods, Results, and Discussion of the manuscript as well as add the red ribbon in Fig. 2 and change the caption accordingly. In addition, throughout the paper we try to specify more precisely which source of uncertainty is meant at the respective point in the text.

1. Section 2. Data and methods (paragraph at the end of Sect. 2.3.4, Line 374):

"However, for certain applications in the insurance industry the tail view of "WISC probabilistic extension" is an important feature of the dataset. The sampling uncertainty of "WISC historic" is too large to provide, for instance, a comparison criterion between two different exceedance frequency curves from different models. Therefore, we propose to illustrate the probabilistic content of "WISC probabilistic extension" by using bootstrapping of all probabilistic damage events. In this way, a "probabilistic envelope" around the best-guess exceedance frequency curve can be determined (see also Sect. 2.4.2). This way of illustration shows how the problem could be addressed in practice, knowing well that it does not illustrate the full uncertainty. In contrast to the sampling uncertainty, the probabilistic envelope could represent something like the "represented uncertainty". In the approach applied, we firstly bootstrapped (random sampling with replacement, number of samples = 100) the historic damage events and then used these samples to create an ensemble of probabilistic damage event sets. Secondly, for each new probabilistic damage event set, we bootstrapped (number of samples = 20) randomly the equivalent of 500 years of windstorm events and built an exceedance frequency curve for each sample. From this set of double-bootstrapped damage event sets (total number of samples = 2000), we then calculated the span between the 5th percentile to the 95th percentile for each exceedance frequency to illustrate the envelope of the probabilistic content."

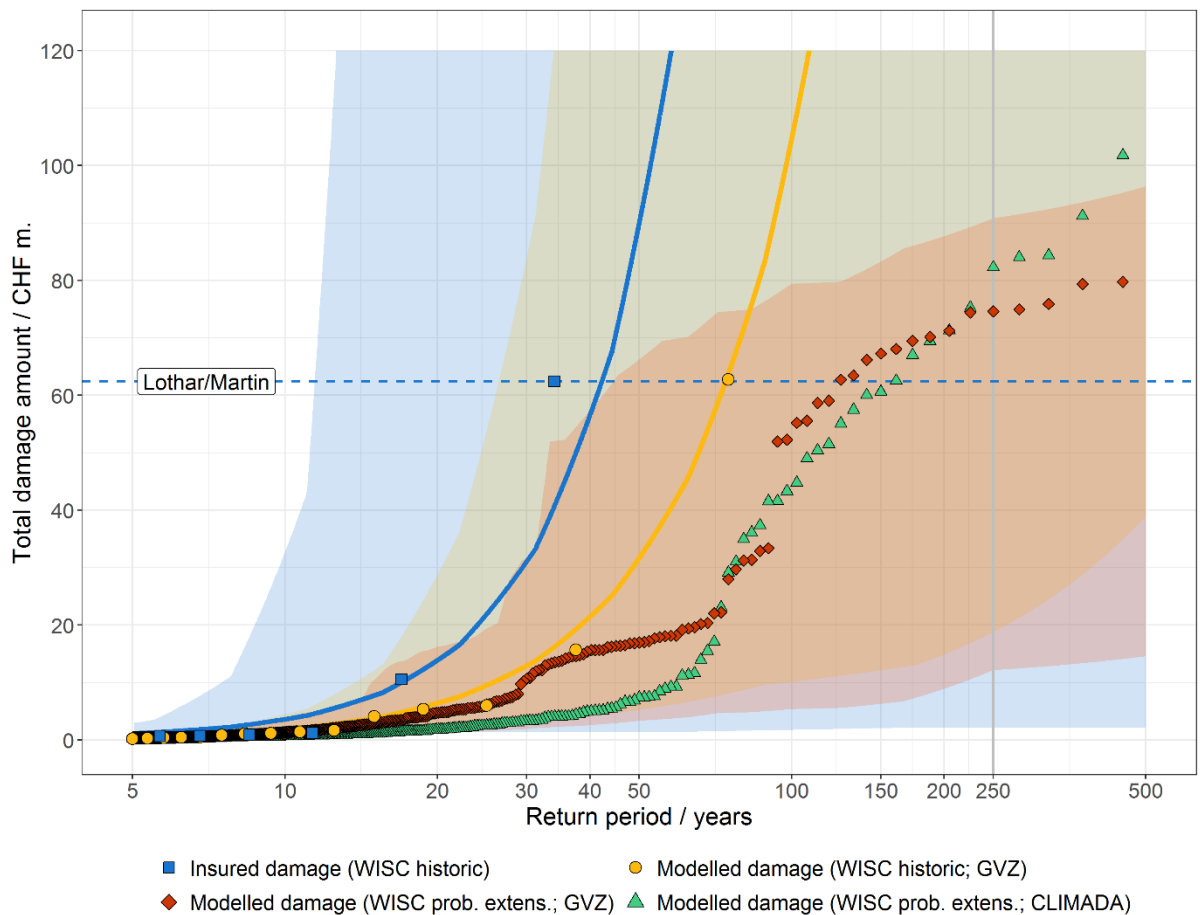*2. Section 3. Results (paragraph at the end of Sect. 3.3, Line 426):*

"The red ribbon in Fig. 2 shows a possibility to illustrate the probabilistic envelope for the modelled damages based on "WISC probabilistic extension" and the GVZ damage model, according to a bootstrapping approach as described in Sect. 2.4.3. As expected, the probabilistic envelope for "WISC probabilistic extension" is much smaller than the range of sampling uncertainty for "WISC historic" (yellow ribbon)."

3. Section 4. Discussion (Line 519):

128 **"The fact that the probabilistic envelope for the modelled damages based on "WISC**
129 **probabilistic extension" (red ribbon in Fig. 2) does not cover the full range of the**
130 **sampling uncertainty for the modelled damages based on "WISC historic" (yellow**
131 **ribbon) shows two things: on the one hand, it shows the tail view, which is possible with**
132 **the help of "WISC probabilistic extension" for certain applications in the insurance**
133 **industry for instance; on the other hand, it reveals the limitations of the statistical**
134 **perturbation, which is used in the generation of "WISC probabilistic extension", to fully**
135 **represent the sampling uncertainty of the underlying historic data. Despite this**
136 **mismatch, […]. In future studies, the information from dynamical models, which are**
137 **run for many model years, would help to further reduce the sampling uncertainty**
138 **compared to this study."**

139 *4. Figure 2 (Line 795):*

140 *The red ribbon is added and the caption is changed accordingly.*

141

142   **"Figure 2: […] The red ribbon shows the probabilistic envelope for the modelled**

143   **damages based on "WISC probabilistic extension" and the GVZ damage model**

144   **computed by applying a bootstrapping approach as described in Sect. 2.4.3. […]"**

145   The remaining two discussion topics in the review (the role of the loss uncertainty due to the vulnerability

146   and the different input exposures) has also been addressed thoroughly and I consider them clarified.

1 **Comparing an insurer's perspective on building damages with**
2 **modelled damages from pan-European winter windstorm event**
3 **sets: a case study from Zurich, Switzerland**

4 Christoph Welker[1], Thomas Röösli[2, 3], David N. Bresch[2, 3]

5 [1] GVZ Gebäudeversicherung Kanton Zürich, Zurich, Switzerland
6 [2] Institute for Environmental Decisions, ETH Zurich, Zurich, Switzerland
7 [3] Federal Office of Meteorology and Climatology MeteoSwiss, Zurich, Switzerland

8 *Correspondence to:* Thomas Röösli (thomas.roeoesli@usys.ethz.ch)

9 **Abstract**

10 With access to claims, insurers have a long tradition of being knowledge leaders on damages caused by e.g.
11 windstorms. However, new opportunities have arisen to better assess the risks of winter windstorms in Europe
12 through the availability of historic footprints provided by the Windstorm Information Service (Copernicus
13 WISC). In this study, we compare how modelling of building damages complements claims-based risk
14 assessment. We describe and use two windstorm risk models: an insurer's proprietary model and the open
15 source CLIMADA platform. Both use the historic WISC dataset and a purposefully-built, probabilistic hazard
16 event set of winter windstorms across Europe to model building damages in the canton of Zurich, Switzerland.
17 These approaches project a considerably lower estimate for the annual average damage (CHF 1.4 million),
18 compared to claims (CHF 2.3 million), which originates mainly from a different assessment of the return period
19 of the most damaging historic event Lothar/Martin. Additionally, the probabilistic modelling approach allows
20 assessing rare events, such as a 250-year return period windstorm causing CHF 75 million damages, including
21 an evaluation of the uncertainties. Our study emphasises the importance of complementing a claims-based
22 perspective with a probabilistic risk modelling approach to better understand windstorm risks. The presented
23 open source model provides a straightforward entry point for small insurance companies.

24 **1   Introduction**

25 Severe windstorms are responsible for widespread socio-economic impacts such as damage to buildings,
26 structures, transport networks, forests, and even loss of lives. Windstorms represent one of the most damaging
27 natural hazards in many parts of the world, not least in Switzerland (Imhof, 2011). In the densely populated
28 canton of Zurich, which is located in north-eastern Switzerland, windstorms are among the most destructive
29 natural hazards: building damages due to windstorms amount to 30 % of the total amount of building damage
30 from natural hazard in this region. For comparison, damages due to hailstorms and flooding amount to 41 % and
31 28 %, respectively (all numbers from 2018; GVZ annual report, 2018; Schadenstatistik VKG, 2020).

32 In general, the impact of a windstorm in terms of building damages depends on the severity of associated
33 surface winds and gusts as well as on the exposed values and the respective vulnerability (i.e., damage
34 susceptibility) of the buildings being subject to the hazard − with both building stock and vulnerability changing
35 over time. High wind speeds cause large pressure and suction effects, which in turn are responsible for damage
36 to the roof and the building facade. Damaging winds and violent gusts in the canton of Zurich are mainly due to

1

37   the passage of large-scale extratropical cyclones and their associated fronts during autumn and winter as well as

38   due to mostly local convective storms during summer. Winter windstorms typically cause widespread minor

39   building damages summing up to large amounts, whereas it is not unusual that summer convective storms cause

40   major damages of only a few buildings due to locally very high wind speeds.

41   The cantonal building insurance GVZ compulsorily insures all buildings in the canton of Zurich (with a few

42   exceptions) against damage due to natural hazards and fire: i.e. in total around 300'000 buildings with a total

43   sum insured of around Swiss Francs (CHF) 500 billion (in 2018). GVZ is an independent institution of the

44   canton of Zurich under public law (GVZ homepage, 2020).

45   Windstorm damage events in the canton of Zurich have been recorded in GVZ's database since 1981. For

46   example, windstorm Lothar on 26 December 1999 caused total insured building damages of around

47   CHF 60 million and is by far the most extreme windstorm event in the database. Second largest is windstorm

48   Burglind on 3 January 2018 (Scherrer et al., 2018), which caused total insured building damages of more than

49   CHF 14 million. The most extreme summer damage event in GVZ's record is due to a very local, but extremely

50   intense convective storm on 2 August 2017 with measured maximum gusts of more than 180 km/h in the

51   lowlands, which caused total insured building damages of approximately CHF 4 million. Even though small-

52   scale convective storm events are potentially hazardous, in this study we focus on large-scale winter windstorms

53   only, which were responsible for around three quarters of all insured windstorm damages in the canton of Zurich

54   since 1981.

55   Extreme damage events such as those caused by Lothar or even stronger windstorms are rare by definition. For

56   risk assessment, solid estimates of the probability of occurrence of such events are absolutely essential and

57   GVZ's claims data of almost 40 years provides a too short observational period which leads to a large sampling

58   uncertainty. A larger sample of events is needed for which at least quantitative meteorological data and if

59   possible damage data at ideally high spatiotemporal resolution are available (e.g., Haas and Pinto, 2012).

60   Observational damage data are generally sparse and incomplete for historic windstorms in Switzerland (Stucki

61   et al., 2014). Instead, societal actors often use modelled impacts to manage their risk. Insurance and reinsurance

62   companies apply impact models for their pricing and governments use modelled risk for option appraisal (e.g.,

63   The Economics of Climate Adaptation Working Group, 2009; Bresch, 2016). Additionally, the information is

64   needed for climate-related financial disclosure (Surminski et al., 2020). However, only very few impact models

65   are available open source and free access for users both in the scientific as well as public or private domain.

66   Typically, risk is modelled as a combination of hazard, vulnerability, and exposure (IPCC, 2014). The hazard

67   part is the best understood and research culminated in open datasets of historic windstorm events (Roberts et al.,

68   2014; WISC products, 2019), whereas maximum wind gust speeds are frequently used as hazard component to

69   assess windstorm risk (e.g., Klawa and Ulbrich, 2003). Vulnerability has been covered by many studies and

70   reviews (e.g., Della-Marta et al., 2010; Schwierz et al., 2010; Feuerstein et al., 2011; Prahl et al., 2015; Koks

71   and Haer, 2018). There are many theoretical learnings from these studies, but an implementation in a

72   comprehensive open source and easy access risk assessment model is still missing. Detailed exposure data are

73   generally not publicly available and many societal actors have their own detailed view on exposure and do not

74   need to rely on a publicly available dataset. There are open, spatially explicit datasets available based on the

75 distribution of nightlight and population (Eberenz et al. 2019), based on the Gross Domestic Product (GDP;

76 Geiger et al. 2018), or on building data from OpenStreetMap (Koks and Haer, 2018). The sparse availability is

77 why in some research studies loss ratios were used instead of information on exposure (Donat et al., 2011).

78 Using the modelling approach for Switzerland, Welker et al. (2016) applied the methods presented first by

79 Stucki et al. (2015) to a sample of more than 80 high-impact winter windstorms that affected Switzerland in

80 1871-2011. The approach involves the dynamical downscaling of the Twentieth Century Reanalysis (20CR)

81 using the Weather Research and Forecasting (WRF) model. The calculated windstorm footprints served as input

82 for the modelling of economic damages using a precursor of the open source impact model CLIMADA

83 (CLIMate ADAptation; Aznar-Siguan and Bresch, 2019a). CLIMADA was successfully applied in several other

84 studies for the purpose of risk assessment and quantification of socio-economic impacts (e.g., Della-

85 Marta et al., 2010; Schwierz et al., 2010; Raible et al., 2012; Reguero et al., 2014; Gettelman et al, 2018; Walz

86 and Leckebusch, 2019).

87 To increase the sample of windstorm footprints available for risk assessment, insurance and reinsurance

88 companies often combine observed windstorm footprints as far as available with synthetic footprints generated

89 by stochastic or dynamic atmospheric models. In this way, they obtain a more comprehensive view on risk.

90 The Windstorm Information Service (WISC) of the Copernicus Climate Change Service aims to provide a

91 consistent and open database of hazard data to assess the risk of windstorms in Europe for all kinds of players in

92 the insurance sector and beyond. The centrepiece of the WISC dataset are wind gust footprints at high spatial

93 resolution of approximately 4.4 km for, on the one hand, a historic hazard event set of around 140 European

94 winter windstorms in 1940-2014 and, on the other hand, a synthetic hazard event set of around 23'000 events.

95 Similar to the predecessor project Extreme Windstorms Catalogue (XWS; Roberts et al., 2014), the WISC

96 historic hazard event set contains windstorms that hit Europe, but provides the corresponding wind gust

97 footprints at improved spatial resolution and covers more windstorms over a period longer than the claims

98 database available to most insurance companies. This makes it possible to reduce the sampling uncertainty of

99 the risk assessment. The windstorm hazard event sets as provided by WISC form an independent database to

100 validate and further develop existing European winter windstorm models. The dataset can be used for both pan-

101 European analyses and local analyses, as shown in this study.

102 Using the WISC historic hazard event set allows GVZ in a way to "re-check" historic events. By means of the

103 synthetic hazard event set, the tail of the hazard and damage distributions should be investigated. However,

104 Röösli et al. (2018) found that the synthetic hazard event set is not suitable for this purpose. Therefore, we

105 propose instead a probabilistic windstorm hazard event set based on a method described in

106 Schwierz et al. (2010) to overcome the shortcomings of the WISC synthetic hazard event set. This new

107 probabilistic hazard event set of around 4'300 events contains windstorms from the WISC historic hazard event

108 set altered by various perturbations. As discussed in this study, such a statistical perturbation is based on the

109 same observational period as the WISC historic hazard event set and therefore cannot reduce the sampling

110 uncertainty.

111 This study shows how GVZ uses both the WISC dataset and the new probabilistic hazard event set for assessing

112 the potential building damage and risk due to extreme windstorm events, including an evaluation of the

3

113　uncertainties of such assessments. A relationship between wind gust speed in the affected region of the canton
114　of Zurich and associated building damages is found, which allows for a rapid, straightforward estimation of
115　damage directly after the occurrence of extreme, unprecedented windstorms. This study further shows how GVZ
116　was able to improve its windstorm risk assessment on the basis of the WISC dataset and the new probabilistic
117　hazard event set, and could serve as an example for other players in the insurance sector or other societal actors
118　in Switzerland and in the rest of Europe. At the same time, this study also illustrates selected limitations of the
119　WISC dataset.

2　Data and methods

121　After a description of the insurance claims data (Sect. 2.1) and the windstorm hazard event sets used (Sect. 2.2),
122　we introduce the GVZ and the CLIMADA risk assessment models applied for damage modelling (Sect. 2.3) and
123　conclude this section with a brief recapitulation of the risk assessment metrics employed in this study
124　(Sect. 2.4).

2.1　Insurance claims data

126　The windstorm damages of past events are recorded in a proprietary database of GVZ. It consists of almost
127　40 years of insurance claims data, in total more than 84'000 single wind damage records. From this database all
128　the events relevant for this study were selected by following the event definition of the windstorm event set
129　"WISC historic" (Sect. 2.2.1). In total, 18 events are associated with WISC windstorms based on that definition
130　(see also Table 1). Due to the nature of the database, only the damage reports actually insured by GVZ were
131　considered. The insurance claims data allow GVZ to assess the risk for its own portfolio by analysing frequency
132　and severity of past damages, i.e. to assess its risk due to winter windstorm events with a return period smaller
133　than 40 years. Additional information can help GVZ to put their recorded damages into reference and to get a
134　better estimate of the risk of events with a return period larger than the 40 years of experience.

135　For the sake of comparability, the insured damages had to be normalised to present-day exposure levels. In this
136　study, the applied normalisation considers the general inflation on the basis of the Zurich construction price
137　index (2020). Hereinafter, both insured and modelled windstorm damages are including occasional deductibles
138　− so-called "gross damages", to ease comparison.

2.2　Windstorm hazard event sets

140　Atmospheric models provide information about winter windstorm events that can be used as hazard component
141　in a risk assessment model. WISC published several hazard datasets each containing a set of windstorm events
142　and providing the maximum wind gust per geographic location per event. We used the historic windstorm
143　footprints (Sect. 2.2.1) and constructed a probabilistic extension based on it (Sect. 2.2.3). In addition, we derived
144　wind gust footprints from measurements for a selection of present windstorm events (Sect. 2.2.4). The additional
145　windstorm hazard event sets published by WISC, that are however not considered in this study, are briefly
146　summarised in Sect. 2.2.2.

4

2.2.1 Historic windstorm hazard event set

The historic windstorm hazard event set − denoted "WISC historic" − contains wind gust footprints for around 140 winter windstorm events in Europe in 1940-2014 (i.e., 75 modelled years in total). The events were selected, on the one hand, based on the high damage they caused and, on the other hand, because of their high intensity in meteorological terms (i.e., high vorticity). Because of this pan-European perspective, the dataset is not necessarily specific to windstorms in the canton of Zurich. Nevertheless, the high-impact windstorms Lothar/Martin (26–28 December 1999) and other intense windstorms such as Vivian/Wiebke (26 February– 1 March 1990) are included.

The windstorm footprints were computed by running the UK Met Office Unified Model (MetUM; Davies et al., 2005) at approximately 4.4 km resolution with ERA-20C reanalysis (Poli et al., 2016) and ERA-Interim reanalysis (Dee et al., 2011) as boundary conditions, covering Europe and parts of the North Atlantic. ERA-20C was used for all windstorm events in 1940-1979 and ERA-Interim for all events in 1979-2014.

Each of the footprints is composed of gridded maximum 3-second gusts, with maxima determined for a 72-hour time window. This relatively long time window was chosen, because it is widely used in the insurance sector (WISC products, 2019). However, it also implies that the footprints of directly successive events (i.e., with a time difference of less than 72 hours) such as Lothar (26 December 1999) and Martin (27-28 December 1999) are combinations of the footprints of both successive events. In this study, the WISC windstorm footprints for events that have overlapping time windows are combined to represent one event – as insurance claims data does often not represent the exact time/date of damage either (for various reasons, a key one being reporting uncertainties). This combination is necessary to make sure that a maximum that occurred only once (e.g., the wind gusts reached during Lothar) is only represented once in the hazard event set (as event Lothar/Martin) and is not represented twice (once as Lothar and once as Martin). There are five pairs of windstorms with overlapping time windows in the original dataset that were combined by taking the maximum wind gust of both footprints at each location, giving in total 142 windstorm events (Table 1). The problem of overlapping windstorm footprints and the resulting combination of events could have been prevented by incorporating the geographical information into the event definition. For example, Roberts et al. (2014) aggregated only the wind gusts within a certain radius around the windstorm centre into a footprint to avoid this problem.

The wind gust speeds from "WISC historic" are considered to be realistic compared to observations for areas at sea level (WISC products, 2019). However, with regard to the hilly topography of the canton of Zurich the question arises as to how realistic the underlying model topography is in comparison to the real topography and, as a result, how good the height-dependent wind gust speeds are compared to observational data. Even though this could not be finally clarified in this study since available wind measurements are generally too sparse for historic windstorms in the canton of Zurich, a correction of all the WISC wind gusts in the form of simple correction factors does not seem reasonable and was therefore not applied.

2.2.2 Other WISC hazard event sets

There are two additional windstorm hazard event sets published by WISC, that are however not analysed in detail in this study:

5

184 1.   The operational windstorm hazard event set − denoted "WISC operational" − contains around
185 110 windstorm events in 1979-2017 and thus more recent events than the windstorm hazard event set "WISC
186 historic" used in this study, which contains windstorm events until 2014 only. "WISC operational" is based on a
187 new generation of atmospheric reanalysis, the ERA5 reanalysis (Hersbach and Dee, 2016). As it does not cover
188 the time range 1940-1979 (compared to "WISC historic") it does not complement the recorded damages by
189 providing information about historic events not covered by GVZ's claims database.

190 2.   The synthetic windstorm hazard event set − denoted "WISC synthetic" − was created within the
191 UPSCALE (UK on PRACE - weather-resolving Simulations of Climate for globAL Environmental risk;
192 UPSCALE, 2020) modelling framework and is a physically realistic set of plausible winter windstorm events in
193 the period 1985-2011 based on the climatic conditions of that period. The modelling framework developed five
194 ensembles. The dataset contains wind gust footprints for around 23'000 synthetic windstorms: i.e., three sets of
195 7'660 events each. Each of the three sets covers 135 modelled years. The original idea of the hazard event set
196 "WISC synthetic" was to use wind information from climate models to provide wind gust footprints for winter
197 windstorms in Europe with a return period of 250 years or even higher. However, this hazard event set was not
198 considered because the findings of Röösli et al. (2018) could be replicated in this study, showing that the dataset
199 does not contain the maximum wind gust speeds we would expect from the distribution of the historic
200 windstorm hazard events (Fig. A1) nor the high intensities we would expect from very rare, high-impact
201 windstorm events (Fig. 1).

202 For a detailed description of all unused windstorm hazard events sets provided by WISC, we refer to the
203 documentations available online at WISC products (2019) and WISC hazard event set description (2019).

2.2.3   Probabilistic windstorm hazard extension

205 Based on "WISC historic", we generated an additional probabilistic windstorm hazard event set − denoted
206 "WISC probabilistic extension". By applying a method described in Schwierz et al. (2010), the individual
207 windstorm events in "WISC historic" (parent events) were altered to create 29 altered offspring events by
208 various perturbations: e.g., spatial displacement and by weakening / intensifying the wind speeds (non-altered
209 wind speeds are spatially displaced only). The spatial displacement was undertaken by shifting the respective
210 windstorm footprint by about 20 km to the north, south, west, or east. The wind gust speeds were intensified and
211 weakened by no more than 3 m/s (normally much less) according to the probabilistic alteration of wind speeds
212 in Eq. (1), with a scale parameter $\alpha = 0.0225$ and a power parameter $\beta = 1.15$ (choice explained further below):

$$windspeed_{scenario\ 1} = windspeed_{original} + \alpha * windspeed_{original}^{\beta}$$

$$windspeed_{scenario\ 2} = windspeed_{original} - \alpha * windspeed_{original}^{\beta}$$

$$windspeed_{scenario\ 3} = windspeed_{original} + \alpha * \sqrt[\beta]{windspeed_{original}} \qquad (1)$$

$$windspeed_{scenario\ 4} = windspeed_{original} - \alpha * \sqrt[\beta]{windspeed_{original}}$$

$$windspeed_{scenario\ 5}$$

$$= windspeed_{original} - \frac{\alpha}{2} * windspeed_{original}^{\beta} - \frac{\alpha}{2} * \sqrt[\beta]{windspeed_{original}}$$

213 These newly created "probabilistic" footprints can be viewed as scenarios of plausible windstorms as they only

214 differ slightly from historic events, retaining both the spatial extent and general structure. In countries close to

215 the sea or with a pronounced and high topography, the methodology for creating the probabilistic events might

216 need adaptation to better incorporate the difference in surface roughness and altitude.

217 For using the scenarios in a qualitative risk assessment framework, the probabilistic windstorm footprints can be

218 used as they are, but for a quantitative risk assessment the frequencies of the windstorm footprints need to be

219 estimated. In an effort to assign reasonable frequency estimates to the probabilistic windstorm footprints, we

220 considered the distribution of the historic, pan-European Storm Severity Index (SSI; formula used by Dawkins

221 et al., 2016; further information in Lamb and Frydendahl, 1991; Leckebusch et al., 2008). Similar as in Schwierz

222 et al. (2010), the algorithm of creating the probabilistic windstorm footprints was configured to recreate the

223 cumulative distribution function of a generalized extreme value (GEV) distribution fitted to the historic SSI

224 values. We defined the frequency of all probabilistic windstorm footprints to be equal and to sum up to the

225 frequency of the parent windstorm. We then selected a set of parameters for weakening and intensifying the

226 wind speeds (parameters α and β in Eq. (1)) that resulted in a similar probabilistic distribution of SSI as the

227 extrapolated distribution from the historic SSI values. For the probabilistic hazard event set to best represent the

228 tail of the historic distribution, we determined a combination of α and β, that minimises the difference in the

229 cumulative distribution functions for events that have a return period of > 75 years.

230 "WISC probabilistic extension" includes footprints for 4'118 probabilistic windstorm events, along with the

231 142 original windstorm events in "WISC historic" (Table 1), and provides a basis of an event-based risk

232 assessment for winter windstorms with return periods of around 250 years, a scenario relevant for regulatory

233 requirements in the insurance sector. It is important to note that this method incorporates a lot of uncertainty,

234 including but not limited to the sampling uncertainty of rare events in a relatively short time range (i.e., 75 years

235 in case of "WISC historic").

236 Encouragingly, the hazard event set "WISC probabilistic extension" shows considerably higher wind gust

237 speeds in the canton of Zurich as compared with "WISC synthetic" (Fig. 1). Nonetheless, the maximum wind

238 gust speeds of the most extreme event in "WISC probabilistic extension" are not considerably higher than those

239 of Lothar/Martin, the most extreme event in both "WISC historic" and the insurance claims data.

240 **2.2.4   Observed footprints for current windstorms**

241 Real-time wind gust observations can serve as the hazard part of the damage model for a rapid damage

242 estimation directly after the occurrence of an extreme windstorm event. Such "observed" windstorm footprints

243 can also be used for further validation of GVZ's damage modelling approach (Sect. 2.3). To create such

244 footprints, we used interpolated wind gust measurements in the canton of Zurich based on the Common

245 Information Platform for Natural Hazards (GIN; GIN platform, 2019) for a selection of seven winter

246 windstorms in the years 2017 and 2018. With the exception of winter windstorm Burglind hitting Switzerland

247 on 3 January 2018, the windstorms considered caused only minor damages in the canton of Zurich. The

7

248 individual windstorm footprints are based on a total of around 110 measurement stations in the canton of Zurich
249 and in the immediate vicinity (i.e., buffer zone with a distance of 20 km around the polyline of the canton). For
250 spatial interpolation, we applied an Inverse Distance Weighting (IDW) interpolation with the Shepard method
251 used for weight calculation. In this study, the gridded wind gust footprints derived from measurements have a
252 horizontal resolution of 2 km. The topography of the canton of Zurich is not considered in the applied
253 interpolation method and unquestionably the quality of the derived windstorm footprints could be improved by
254 using a more elaborate interpolation method, which takes account of the topography.

2.3 Damage modelling approaches

256 The windstorm footprints of the different hazard event sets described in the previous section were used as input
257 for damage modelling and GVZ's proprietary windstorm damage model was applied for this (Sect. 2.3.1). In
258 addition, the CLIMADA impact model was used to be able to publish the method used in this study with open
259 data and open source code (Sect. 2.3.2).

260 In both damage models, the extent of damage results from the intensity of the windstorm event (i.e., hazard), the
261 value of the asset (i.e., exposure), and the susceptibility of the asset to damage (i.e., vulnerability). This concept
262 is broadly used and is explained in more detail in Aznar-Siguan and Bresch (2019a). In this study, the
263 windstorm hazard assessment is based on the winter windstorm footprints described in Sect. 2.2. The exposure
264 is the value of the buildings in the canton of Zurich and the vulnerability is described by a functional
265 relationship that defines how much the buildings are damaged at a certain wind gust speed. In both damage
266 models, we use the vulnerability curve of Schwierz et al. (2010). This vulnerability curve combines the damage
267 degree and the percentage of assets affected. Only damage to buildings is estimated. The estimate does not
268 include damage to movable property, damage to infrastructure, nor business interruption.

2.3.1 GVZ damage model

270 The damage estimates in this model are computed using a rather conventional modelling framework and the
271 reduced complexity of the approach allows a well interpretable assessment of the model skill. Normally, GVZ
272 uses its damage model directly after the occurrence of a windstorm event to estimate the expected building
273 damage. Furthermore, GVZ applies the damage model to estimate the damage potential and the risk associated
274 with windstorms with regard to solvency considerations and prevention options. The main points of the
275 modelling approach are described in the following.

276 The initial step is a simple spatial overlay of the gridded maximum wind gust speeds during the respective
277 windstorm event with GVZ's current building stock (from 2018; without sublevel garages, as they are usually
278 not affected by windstorms), where GVZ's proprietary building database with information about e.g. the sum
279 insured of each building and the publicly available building footprints (GIS browser Zurich, 2019) were used.
280 GVZ's insurance penetration in the canton of Zurich is almost 100 %. In the damage model, damage is possible
281 from a wind gust speed of more than 90 km/h, and only buildings affected by such gusts were considered in the
282 following modelling steps.

283 Figure A2 shows the spatial distribution of all insured buildings in the canton of Zurich as well as of the total
284 sum insured at municipal level. The aggregated sum insured for all buildings in the two main cities, Zurich and

8

285 Winterthur (municipal boundaries indicated by blue polygons), accounts for almost 40 % of the total insured
286 value for the entire canton.

287 To estimate the damage in monetary terms, the value of each individual building (i.e., its insured value) was
288 multiplied by the factor "Mean Damage Degree" (MDD, a number between 0 and 1) calculated from the
289 vulnerability curve of Schwierz et al. (2010), where the gust speeds at building level computed in the first step
290 were converted into the corresponding MDD factors. The MDD factors are a non-linear function of the
291 maximum wind gust speed during a windstorm event and are diagrammed in Welker et al. (2016). The same
292 vulnerability curve of Schwierz et al. (2010) is also implemented in the open source impact model CLIMADA
293 (Aznar-Siguan and Bresch, 2019a).

294 In the next step of the damage model, the probability of buildings affected is calculated with a stochastic
295 approach. The respective windstorm event was automatically categorised according to its severity (here,
296 according to the 95th percentile of all gust speeds at building level in the affected region of the canton of
297 Zurich), from which the assumed degree of impact is derived. The degree of impact for the different windstorm
298 categories (i.e., a percentage of total affected buildings for the canton of Zurich, m) was derived from
299 proprietary event damage data from GVZ's database. Then, a random sample of m buildings was selected, with
300 the number m depending on the windstorm's severity. Only buildings with MDD > 0 were considered, i.e. only
301 those buildings with potential damage > 0. For the selected buildings, the amount of damage at building level
302 was summed to obtain the total damage for the entire canton. This procedure of random sampling was repeated
303 1'000 times giving a total damage range for each windstorm event. Unless otherwise stated, for each windstorm
304 the median of the damage distribution is given hereinafter.

2.3.2 CLIMADA impact model

306 The windstorm damage model in the open source risk assessment platform CLIMADA is relying on open data
307 only and that is why it is deviating in some aspects from GVZ's approach described above. As the windstorm
308 hazard component is open, it is identical to the hazard input used in case of the GVZ damage model. The
309 exposure is based on public data instead of GVZ's proprietary portfolio information. CLIMADA uses produced
310 capital for Switzerland published by the World Bank (2018) as the total value of physical assets for Switzerland
311 and further uses a combination of nightlight intensity and population density to create a reliable geographical
312 distribution of the assets (Eberenz et al., 2019). The resulting values are then distributed to building footprints
313 from OpenStreetMap (OpenStreetMap contributors, 2017). Analogous to the GVZ damage model, CLIMADA
314 uses the MDD curve of Schwierz et al. (2010). Instead of a random resampling of affected buildings, the MDD
315 factor is combined with the deterministic factor "Percentage of Assets Affected" (PAA).

316 As the total value of the exposure is different between the GVZ exposure, the CLIMADA exposure, and the
317 exposure used in Schwierz et al. (2010), the MDD and PAA factors might be wrongly scaled for this study. In
318 the CLIMADA model setup used, we adjusted for this by linearly scaling the MDD and PAA factors to reduce
319 the difference of the modelled damages and the insured damages for matching events (i.e., by minimising the
320 root-mean-square deviation, RMSD). This adjustment conserved the shape of the original vulnerability curve.

9

321 The CLIMADA impact model and the GVZ damage model have a different sensitivity to the hazard intensity: in
322 CLIMADA, damage is possible for a wind gust speed of 72 km/h (20 m/s) and above, in the GVZ damage
323 model for 90 km/h (25 m/s) and above.

2.4   Assessment of potential windstorm damage and risk

325 Risk is defined here as the product of the extent of damage and the probability of damage. The probability of
326 damage is driven, on the one hand, by the probability that the building is within the area of high wind gust
327 speeds and, on the other hand, by the return period of the windstorm event. The probability, that the building is
328 within the area of high wind gust speeds is incorporated in the modelled damage amount by the spatially explicit
329 modelling approach and the vulnerability, which includes the percentage of assets affected (in case of
330 CLIMADA). The return period or frequency of windstorm events is derived from the hazard event sets. Return
331 periods express the probability of occurrence of windstorm events (e.g., an event with a return period of 250
332 years is expected on average every 250 years).

333 There are several risk assessment metrics that can be calculated with a set of event damages, which are the main
334 result from the damage modelling described above.

2.4.1   Average annual damage

336 The average annual damage (AAD) is an important risk measure in the insurance industry. It describes the risk
337 from all events reported on an annual basis:

$$AAD = \frac{sum\ of\ all\ event\ damages}{time\ range\ covered\ by\ event\ set} = \sum_{event\ i} event\ damage_i * annual\ frequeny_i \quad (2)$$

2.4.2   Exceedance frequency curve

339 Using the annual frequencies of the events in a hazard event set, it is possible to determine at what frequency a
340 certain damage amount is exceeded. The largest damage amount is exceeded once in the time range covered by
341 the damage event set, the second largest damage amount is exceeded twice, the third one thrice and so on. The
342 exceedance frequency curve shows the damage amount as a function of exceedance frequency. For large
343 damage amounts, this matching typically relies on only a few damage events, which increases the
344 ~~statistical~~sampling uncertainty.

2.4.3   Pareto pricing

346 In the insurance industry, the concept of "Pareto pricing" is a simple approach to represent and extrapolate the
347 distribution of a damage event set to define the price of insurance contracts (Mitchell-Wallace et al., 2017). We
348 imitated this pricing method by fitting a Generalized Pareto Distribution (GPD) to damage event sets using a
349 Maximum Likelihood Estimate (MLE). We do this even though some assumptions in statistical theory are not
350 valid for these datasets (e.g., windstorm damage event sets are clustered which breaks the independence
351 assumption), as we use the GPD only to show the underlying sampling uncertainty. To fit a GPD to a damage
352 event set, only the threshold has to be chosen. We chose a threshold for each damage event set, which results in
353 a parameterised GPD with similar exceedance frequencies for the largest damage amount in the event set. For

354 the insured damages we chose a threshold of CHF 0.4 million and for the modelled damage event set based on
355 "WISC historic" we chose a threshold of CHF 0.1 million. By using the percent point function (the inverse of a
356 cumulative distribution function) on the fitted distributions, an exceedance frequency curve for the fitted
357 distribution was calculated.

358 To illustrate the ~~statistical~~ uncertainty of the exceedance frequency curve, we undertook a resampling and
359 thereby show the sampling uncertainty for each damage event set. In the resampling, we generated 200 random
360 samples from the fitted distribution and used the MLE to fit a GPD to each random sample. The exceedance
361 frequency curves of these resampled distributions illustrate the sampling uncertainty especially for rare events
362 with a high return period. We show the 90-% confidence interval of damage amounts for each exceedance
363 frequency, which spans from the 5th percentile to the 95th percentile of the 200 samples.

364 In case of the damage event set computed on the basis of "WISC probabilistic extension", the uncertainty is best
365 illustrated by the sampling uncertainty of the damage event set based on "WISC historic" for the following
366 reasons. The procedure of computing the hazard event set "WISC probabilistic extension" by statistical
367 perturbation (as described in Sect. 2.2.3) transforms part of the sampling uncertainty of the hazard event set
368 "WISC historic" into an uncertainty of the parameters α and β in Eq. (1). However, this parameter uncertainty is
369 difficult to illustrate, since no combination of α and β could be found which adequately represents the upper and
370 lower boundaries of the sampling uncertainty of the pan-European SSI distribution. Additionally, the sampling
371 uncertainty of "WISC probabilistic extension" no longer represents the same uncertainty as in case of the other
372 damage event sets. Thus, for ~~comparison~~the purpose of comparing the uncertainties of the different damage
373 event sets, we suggest to use the sampling uncertainty of "WISC historic" as best illustration of the uncertainty
374 of "WISC probabilistic extension".

375 However, for certain applications in the insurance industry the tail view of "WISC probabilistic extension" is an
376 important feature of the dataset. The sampling uncertainty of "WISC historic" is too large to provide, for
377 instance, a comparison criterion between two different exceedance frequency curves from different models.
378 Therefore, we propose to illustrate the probabilistic content of "WISC probabilistic extension" by using
379 bootstrapping of all probabilistic damage events. In this way, a "probabilistic envelope" around the best-guess
380 exceedance frequency curve can be determined (see also Sect. 2.4.2). This way of illustration shows how the
381 problem could be addressed in practice, knowing well that it does not illustrate the full uncertainty. In contrast
382 to the sampling uncertainty, the probabilistic envelope could represent something like the "represented
383 uncertainty". In the approach applied, we firstly bootstrapped (random sampling with replacement, number of
384 samples = 100) the historic damage events and then used these samples to create an ensemble of probabilistic
385 damage event sets. Secondly, for each new probabilistic damage event set, we bootstrapped (number of
386 samples = 20) randomly the equivalent of 500 years of windstorm events and built an exceedance frequency
387 curve for each sample. From this set of double-bootstrapped damage event sets (total number of
388 samples = 2000), we then calculated the span between the 5th percentile to the 95th percentile for each
389 exceedance frequency to illustrate the envelope of the probabilistic content.

11

3   Results

3.1   Single events

The damage due to Lothar/Martin is by far the largest windstorm event damage in GVZ's insurance claims database (Fig. A3a): Lothar/Martin caused insured damages of CHF 62.4 million. Lothar/Martin is the most damaging windstorm event in the canton of Zurich in both the 34-years period of insurance claims data as well as in the 75-years period of "WISC historic". The damages modelled with the GVZ damage model range between CHF 58.0 million and CHF 69.0 million, and the median of all modelled damages amounts to CHF 62.7 million (Fig. A3b). For Burglind, the most damaging event of the "observed footprints", the modelled damages range between CHF 10.4 million and CHF 14.5 million, with a median of CHF 12.0 million. For comparison, the insured damages amount to CHF 14.2 million. Thus, damages associated with intense windstorm events like Lothar/Martin or Burglind are very well modelled with GVZ's damage modelling approach, providing confidence in the methodology. For all recorded windstorm events since 1981 (including the additional seven windstorms in 2017 and 2018), the RMSD between the insured damage and the median modelled damage amounts to CHF 2.4 million. Furthermore, the example of Burglind shows that our methodology of creating windstorm footprints on the basis of interpolated wind gust observations (Sect. 2.2.4) is suitable for present and probably also for future windstorm events.

3.2   Average annual damage

The average annual damage (AAD) calculated based on the insured damages (i.e., the mean damage over the observational period of 34 years) is almost twice as high as the AAD computed on the basis of "WISC historic" (Table 2). Several factors contribute to the fact that the AAD is higher for the insured damages than for the modelled damages based on "WISC historic": (i) the occurrence of the very intense event Lothar/Martin, along with other intense events, in the relatively short available period of insurance claims data (Fig. A3a), (ii) the higher damages of events in the 5-year return period range (Table 2), and (iii) the different number of events per year considered. The hazard event set "WISC probabilistic extension" was created to best represent the low-frequency tail of the pan-European SSI and not the full distribution of (high frequency) damages in the canton of Zurich. Nevertheless, the modelled AAD based on the GVZ damage model and "WISC probabilistic extension" is close to the AAD of "WISC historic".

3.3   Assessment of risks due to extreme windstorm events

Figure 2 shows GVZ's windstorm risk assessment of building damage, including uncertainty, on the basis of all available data sources. Based on the insurance claims data only, the return period for the extreme windstorm event Lothar/Martin is estimated to be 34 years (blue squares). Based on "WISC historic", the return period for Lothar/Martin is estimated to be 75 years (yellow dots). Based on the hazard event set "WISC probabilistic extension" and using GVZ's approach for damage modelling, the return period for a damage amount due to Lothar/Martin would be around 125 years (red diamonds). These estimates represent the best guess for each damage event set. It is important to note that the quantified sampling uncertainty of the estimate for the return period of Lothar/Martin based on "WISC historic" (yellow ribbon, 25 years to > 500 years) incorporates both

12

426 the estimate for the insurance claims data (blue ribbon) as well as the estimate based on "WISC probabilistic
427 extension".

428 The extrapolated event damage with a return period of 250 years amounts to about CHF 500 million for
429 "WISC historic" and using the same method for the insured damages the extrapolated 250-year event damage
430 would be even higher, around CHF 2.4 billion (yellow and blue lines in Fig. 2). Contrary to this, the 250-year
431 event damage amounts to only about CHF 75 million in case of the hazard event set "WISC probabilistic
432 extension" (red diamonds). The 90-% confidence interval, which represents the sampling uncertainty of the
433 extrapolation of the damage exceedance frequency, based on "WISC historic" provides a range for the 250-year
434 return period damage of CHF 19 million to CHF 33 billion (yellow ribbon). As "WISC probabilistic extension"
435 is based on the same historic information this sampling uncertainty also applies to its results. At a return period
436 of 250 years, the quantified uncertainty of the estimate based on "WISC historic" incorporates both the estimate
437 for the insurance claims data as well as the estimate based on "WISC probabilistic extension".

438 An interesting feature illustrated in Fig. 2 is that at higher return periods the modelled damages on the basis of
439 "WISC probabilistic extension" increase less strongly compared to the two extrapolations based on the fitted
440 distributions. Evident "jumps" in the modelled damage (e.g., at return periods of approximately 30 years,
441 70 years, and 90 years) result from the discrete categorisation of the individual windstorm events and the
442 assumed degrees of impact, respectively, as applied in GVZ's damage modelling approach (Sect. 2.3.1).

443 The red ribbon in Fig. 2 shows a possibility to illustrate the probabilistic envelope for the modelled damages
444 based on "WISC probabilistic extension" and the GVZ damage model, according to a bootstrapping approach as
445 described in Sect. 2.4.3. As expected, the probabilistic envelope for "WISC probabilistic extension" is much
446 smaller than the range of sampling uncertainty for "WISC historic" (yellow ribbon).

447 **3.4   Reproducibility of the results using CLIMADA**

448 In general, GVZ's proprietary windstorm damage model is suitable for correctly simulating building damage in
449 the canton of Zurich (see Fig. 3, Fig. A3, and Sect. 3.1). Using the calibrated CLIMADA impact model for
450 windstorm damage modelling is also suitable and the corresponding RMSD amounts to CHF 1.5 million for all
451 recorded windstorm events since 1981 for which WISC wind gust footprints are available (excluding the
452 additional windstorms in 2017 and 2018). The statistics in Table 2 calculated using the GVZ damage model
453 were also calculated using the CLIMADA impact model and the results can be found in Table A1. In summary,
454 it can be stated that the setup of the two damage models applied works well and e.g. replicates the order of the
455 events, provides a reasonable modelled damage for historic events (compared to insurance claims data), and
456 both RMSD are sufficiently good.

457 The exceedance frequency curve of the modelled damages based on "WISC probabilistic extension" and the
458 CLIMADA impact model (green triangles in Fig. 2) show in general lower values compared to the damage
459 modelling using the GVZ approach (red diamonds), in particular for return periods between 30 and 70 years.
460 This difference is also reflected in the scatter plots in Fig. 3, where in Fig. 3a the GVZ damage model shows an
461 overestimation of the damage amount due to the windstorm event Vivian/Wiebke (with insured damage of
462 approximately CHF 11 million), whereas the CLIMADA impact model shows an underestimation for the same

13

463 event. The reason for this over- and underestimation of the damage in case of events such as Vivian/Wiebke
464 could be due to the hazard or exposure part of the respective model, but is more likely due to the applied
465 vulnerability curve itself. Apparently, the two damage models perform differently for windstorm events in a
466 medium intensity category. This difference between the two models also becomes evident regarding the AAD
467 risk metric: the AAD of the CLIMADA impact model with "WISC historic" amounts to CHF 1.1 million
468 (Table A1) and is thus almost a third smaller than the AAD associated with the GVZ damage model
469 (CHF 1.4 million). In addition, the curve of the modelled damages is much smoother in case of CLIMADA
470 (Fig. 2), which can be explained by the fact that in CLIMADA the smooth curve of the PAA factors is used.
471 This shows the importance of the applied vulnerability curve in the presented damage modelling approach.

472 **3.5   Rapid damage estimation**

473 Rapid damage estimation directly after a windstorm event is very useful for insurance companies to get a first
474 rapid assessment of the damage to be expected and to e.g. assign their staff accordingly. For current windstorm
475 events, the GVZ does this using its damage model and the wind gust footprints based on "observed footprints"
476 (Sect. 2.2.4). The 95th percentile of the wind gust speeds at building level in the affected region of the canton of
477 Zurich, which is also used in GVZ's damage model to categorise windstorm events (Sect. 2.3.1), is used as a
478 rapid indicator of the range of possible damages. This process is illustrated in Fig. 4. With the help of the dataset
479 "WISC probabilistic extension", assessments can also be made about potential damages from unprecedented,
480 extreme windstorm events. The uncertainty of the damage assessment for such extreme events can be visualised
481 by the large number of available (extreme) events. In total, "WISC probabilistic extension" contains 17 events
482 which are potentially more damaging than Lothar/Martin. A (modelled) total damage amount of more than
483 CHF 96 million is associated with the most extreme windstorm event in "WISC probabilistic extension"
484 (Fig. 1). Thus, this windstorm is potentially about 1.5 times as damaging as Lothar/Martin.

485 Figure 4 further shows, by the length of the red bars, the stochastic component in GVZ's damage modelling
486 approach, which tries to approximate the random selection as not every building is equally affected during a
487 windstorm event (Sect. 2.3.1). The range of modelled damages (length of red bars) increases with increasing
488 wind gust speed. On the other hand, the quotient of the range of modelled damages and the median of the
489 damage distribution (red points) generally decreases with increasing wind gust speed. "Jumps" in the modelled
490 damage (e.g., for wind gust speeds lower than 126 km/h) again result from the discrete categorisation of the
491 individual windstorm events in the GVZ damage model.

492 The absolute difference between the modelled damage amount and the corresponding value of the regressed
493 relationship (red points and solid red line in Fig. 4) generally increases with increasing wind gust speed.
494 Accordingly, the number of available wind gust footprints decreases with increasing wind gust speed.

495 **4   Discussion**

496 Any information about the historic risk of winter windstorms in the canton of Zurich contains the record of the
497 event Lothar/Martin. As this is the most damaging event in the record by far, the general risk assessment is
498 connected to the assessment of the return period of such an event damage, which will always be uncertain. We
499 argue that the return period based on the historic windstorm footprints (75 years) is much more reliable than the

14

500 return period based on the insured damage record (34 years). Well knowing that the two estimates each have
501 overlapping uncertainties, the estimates do not contradict each other. Rather the estimates, as best guesses, can
502 inform varying deterministic risk views. Other information, like the return period of Lothar/Martin's damage
503 amount based on "WISC probabilistic extension" and an independent catalogue of historic windstorms in
504 Switzerland by Stucki et al. (2014) suggest that the return period of such a damage amount could be even rarer
505 than 75 years. This clearly shows the added value that GVZ achieves in its risk assessment through applying the
506 WISC wind data compared to using insurance claims data only − and, above all, through the additional dataset
507 "WISC probabilistic extension". The return period of extreme windstorm events such as Lothar/Martin can now
508 be assessed more reliably.

509 The windstorms Lothar and Martin affected, in addition to Switzerland, in particular France, Belgium,
510 Luxembourg, and Germany. The original industry damage associated with Lothar and Martin amount to
511 approximately EUR 5.8 billion and EUR 2.5 billion, respectively (PERILS, 2020). The return period for
512 exceeding the damage amount due to Lothar alone in all of Europe was estimated to be 15 years by
513 Munich Re (2002) and the return period for the cluster of the three windstorms in December 1999 Anatol
514 (3 December 1999), Lothar, and Martin was estimated to be between 22 and 45 years
515 (Renggli and Zimmerli, 2016). This study shows that it is important to make a distinction between the return
516 period of an event like Lothar/Martin in all of Europe and the return period of this event locally, in a relatively
517 small region. The damage modelling shown in this study, using the event set "WISC historic" and the local
518 exposure information, enables a much more reliable derivation of the return period specific to GVZ than the
519 existing scientific work is able to provide.

520 Based on "WISC historic" and the GVZ damage model, the average annual damage for building damages in the
521 canton of Zurich amounts to CHF 1.4 million according to our calculation and we argue that this is the best
522 available estimate for the AAD. However, this estimation is still uncertain due to the high sampling uncertainty,
523 the uncertainty associated with the assessment of the event Lothar/Martin, and the uncertainty with regard to the
524 damage modelling itself. For comparison, in the last 10 years GVZ has experienced yearly damage from all
525 natural hazards of CHF 16 million and additionally yearly damage by fire of CHF 42 million (all numbers from
526 2018; GVZ annual report, 2018). Compared to the risk from these hazards, the estimated AAD from winter
527 windstorms of CHF 1.4 million is relatively small. However, the occurrence of windstorm events such as
528 Vivian/Wiebke, Lothar/Martin, and Burglind has shown that single windstorms are able to cause huge damage
529 amounts and they are consequently an important causal element when assessing capital requirements.

530 Insurance companies undertake their business under a strict regulatory environment, and having enough capital
531 to cover rare events is one of the regulatory requirements. The damage amount reached on average every
532 250 years is an often-mentioned indicator for such a rare event. However, the insured damages and also the
533 modelled damages based on "WISC historic" do not span a long enough period by far to make an empirical
534 prediction of a damage amount with a return period of 250 years. All methods of extrapolation from these
535 datasets suffer from the sampling uncertainty (shown as confidence intervals in Fig. 2). The hazard event set
536 "WISC probabilistic extension" uses the distribution of pan-European SSI values to create a set of probable
537 events with higher return periods than "WISC historic". The uncertainty of the return periods of such events
538 cannot however cannot considerably be reduced compared to "WISC historic", because it relies on the same

15

historic information. ~~In future studies, the information from dynamical models, which are run for many model years, would help to further reduce this uncertainty. Despite the uncertainty~~ The fact that the probabilistic envelope for the modelled damages based on "WISC probabilistic extension" (red ribbon in Fig. 2) does not cover the full range of the sampling uncertainty for the modelled damages based on "WISC historic" (yellow ribbon) shows two things: on the one hand, it shows the tail view, which is possible with the help of "WISC probabilistic extension" for certain applications in the insurance industry for instance; on the other hand, it reveals the limitations of the statistical perturbation, which is used in the generation of "WISC probabilistic extension", to fully represent the sampling uncertainty of the underlying historic data. Despite this mismatch, it can nevertheless be important to study the sensitivity of the 250-year return period damage to changes in the portfolio (like growth or changed building codes), changes in the deductible or other changes. "WISC probabilistic extension" provides windstorm footprints of events with a return period of 250 years (and more), that allow the modelling of damages with changes in the exposure or the vulnerability. In future studies, the information from dynamical models, which are run for many model years, would help to further reduce the sampling uncertainty compared to this study.

It comes as no surprise that the choice of the vulnerability curve in the damage modelling approach applied strongly influences the results of the damage estimation (e.g., Koks and Haer, 2018), and unsurprisingly no optimal "one-size-fits-all" vulnerability curve exists. Every damage model behaves differently, not least because different vulnerability curves are used and each of the damage models has been calibrated differently. The vulnerability curve of Schwierz et al. (2010) is based on movable property and building damages associated with European winter windstorms. The rather general function does not make a distinction between building types, in contrast to other available functions (e.g., Feuerstein et al., 2011). For a modelling setup with focus on the hazard, the vulnerability curve of Schwierz et al. (2010) is however suitable and was successfully applied in earlier studies (e.g., Stucki et al., 2015; Welker et al., 2016). The function does not require detailed information regarding the values at risk, which is certainly an advantage for such insurance and reinsurance companies that do not have detailed exposure data for their damage modelling. A disadvantage of the used vulnerability curve is that it does not implicitly provide a quantification of the uncertainty as a probabilistic vulnerability curve would (e.g., Heneka et al., 2006; Prahl et al., 2012). The quantification of the uncertainty of exposure and vulnerability information was generally omitted in this study to focus on the comparison of the claims and hazard datasets. But of course, for comparison of the presented risk numbers with other studies the uncertainty of the vulnerability and exposure information play a bigger role. The vulnerability assumed in this study and the corresponding hazard intensity only considers the maximum gust speeds during an event and not the duration of high wind gusts within a windstorm event, which can however have a major impact on the damage to be expected. Taking the windstorm duration into account (e.g., Etienne and Beniston, 2012) could improve our damage modelling, and it is planned to implement this in a future version of GVZ's damage model. Furthermore, it is not considered that buildings are partially adapted to local wind conditions (e.g., multi-storey buildings or exposed buildings located on mountain tops).

Not every building is equally affected during a windstorm event. To take that into account, in the GVZ damage model a random resampling of affected buildings was applied according to an assumed degree of impact (red bars in Fig. 4). The assumed degree of impact was derived according to the respective severity category of the

578 windstorm. This severity categorisation and the assumed degrees of impact are inevitably relatively rough in
579 GVZ's current model setup, because the assumptions are based on insurance claims data from only a few past
580 windstorm events in the canton of Zurich. With every further windstorm, these assumptions will however
581 become more reliable in the future. In contrast, the deterministic PAA values (Schwierz et al. 2010), as used in
582 the CLIMADA impact model, are much smoother and thus allow a smooth damage modelling (Fig. 2).
583 However, these values are not specific for windstorms in the canton of Zurich and they do not allow a stochastic
584 sampling as in GVZ's damage modelling approach.

585 The rapid estimate of the damage potential in the event of extreme, unprecedented windstorm events shown in
586 Fig. 4 is just one example of how the WISC data and in particular the additional damage event set
587 "WISC probabilistic extension" can be used for insurance applications. The idea was to be able to make a
588 statement about the damage to be expected simply based on available wind observations in the area of the
589 canton of Zurich. It is always important for insurance companies to be able to give a damage assessment as
590 rapidly as possible after an event, not least when it comes to media inquiries. However, one should keep in mind
591 that the uncertainty shown does not incorporate the full uncertainty of the damage estimate, but rather the
592 uncertainty that results from the random selection as not all buildings are affected equally during a windstorm
593 event. In a future study, it would be interesting to quantify the full uncertainty of the rapid damage estimate.

594 Not least, the WISC wind data enable insurance companies to evaluate the variability and long-term changes of
595 winter windstorms and their associated damage since 1940. Besides a marked interannual and decadal-scale
596 variability of windstorms in the canton of Zurich, we find a tendency for more intense windstorms since
597 approximately mid of the 1980s (Fig. A3d). One possible reason for this positive trend is that "WISC historic"
598 consists of two "parts" with different databases: until 1979, the ERA-20C reanalysis (Poli et al., 2016) was used
599 for downscaling, followed by the ERA-Interim reanalysis (Dee et al., 2011). Furthermore, a change in the large-
600 scale, atmospheric dynamics has been observed in recent decades, which was conducive to increased winter
601 windstorm activity and intensity in Switzerland (Welker and Martius, 2015). This change was accompanied by
602 an atmospheric circulation pattern resembling a southeastwardly displaced winter North Atlantic Oscillation
603 (NAO) pattern. Which of the two reasons is dominant for the found positive tendency in winter windstorm
604 intensity and associated damages in the canton of Zurich could not be finally clarified in the present study.
605 Furthermore, how winter windstorm activity and intensity in mid-latitude Europe will change in a future warmer
606 climate is still uncertain (Catto et al., 2019).

607 **5   Conclusion**

608 This study is an example of how a regional building insurance company in Switzerland uses the open database
609 of European windstorm event sets provided by WISC in combination with a probabilistic extension for their
610 assessment of potential building damages and risks as a result of extreme winter windstorm events, including an
611 evaluation of the uncertainties. The windstorm event Lothar/Martin in December 1999 is the most damaging
612 event in both the insurance claims data and "WISC historic" (damage of more than CHF 60 million). The
613 average annual damage for building damages in the canton of Zurich is CHF 1.4 million, computed based on
614 "WISC historic" and the GVZ damage model.

17

615 Both the insurance claims data and the modelled building damages based on "WISC historic" are rather
616 unsuitable for evaluating rare windstorm damage events with return periods considerably exceeding the
617 observational period. The new hazard event set "WISC probabilistic extension" projects a damage amount of
618 approximately CHF 75 million for a return period of 250 years, while the uncertainty for an extrapolation to
619 such return periods is still very large. However, the probabilistic hazard event set allows for testing the
620 sensitivity of the risk to e.g. changes in the insurance portfolio or in the insurance condition (e.g., the deductible)
621 for events of a higher intensity than the observed historic events.

622 Our analysis is implemented in GVZ's proprietary windstorm damage model as well as in the open source risk
623 assessment platform CLIMADA (Bresch and Aznar-Siguan, 2019a). This guarantees scientific reproducibility
624 and offers insurance companies and other societal actors in Switzerland and the rest of Europe the opportunity to
625 apply the shown methodology to their own portfolio with a low entry threshold. This study illustrates how open
626 climatological data and open source damage models can be used to assess windstorm risks in Europe and how
627 this approach complements risk assessments based on proprietary insurance claims data only.

628 There is a growing societal need for physical risk disclosure, not least in the context of the Task Force for
629 Climate-related Financial Disclosure (TCFD; Surminski et al., 2020). The presented methodology, in particular
630 the combination of the WISC hazard data with the open source CLIMADA platform, can be used for such a
631 disclosure report.

632 **Code availability and data availability**

633 The scripts reproducing the main results of the paper and the figures are available under
634 https://github.com/CLIMADA-project/climada_papers. The probabilistic hazard event set "WISC probabilistic
635 extension" for each European country is made available for download under https://doi.org/10.3929/ethz-b-
636 000406567 (Röösli and Bresch, 2020).

637 CLIMADA is openly available at GitHub (https://github.com/CLIMADA-project/climada_python; Bresch and
638 Aznar-Siguan, 2019a) under the GNU GPL license (GNU operating system, 2007). The documentation is hosted
639 on Read the Docs (https://climada-python.readthedocs.io/en/stable/; Aznar-Siguan and Bresch, 2019b) and
640 includes a link to the interactive tutorial of CLIMADA. CLIMADA v1.4.1 was used for this publication, which
641 is permanently available at the ETH Data Archive: http://doi.org/10.5905/ethz-1007-252 (Bresch et al., 2020).

642 **Author contribution**

643 CW and TR share first co-authorship and contributed equally to defining the case study, performing the
644 analyses, writing the article, and participating in the review process. CW developed the GVZ damage model and
645 TR generated the hazard event set "WISC probabilistic extension". DNB contributed to writing the article,
646 conceptualised CLIMADA, and over-saw its implementation in Python, based on the previous MATLAB
647 implementation by himself.

18

658 **References**

659 Aznar-Siguan, G. and Bresch, D. N.: CLIMADA v1: a global weather and climate risk assessment platform,

660   Geosci. Model Dev., 12, 3085-3097, https://doi.org/10.5194/gmd-12-3085-2019, 2019a.

661 Aznar-Siguan, G. and Bresch, D. N.: CLIMADA_python documentation, https://climada-

662   python.readthedocs.io/en/stable/, last access: 17 July 2019, 2019b.

663 Bresch, D. N.: Shaping Climate Resilient Development – Economics of Climate Adaptation, in: Climate Change

664   Adaptation Strategies – An Upstream-downstream Perspective, edited by: Salzmann, N., Huggel, C.,

665   Nussbaumer, S., and Ziervogel, G., Springer, Cham, 241-254, https://doi.org/10.1007/978-3-319-40773-

666   9_13, 2016.

667 Bresch, D. N. and Aznar-Siguan, G.: CLIMADA-python, https://github.com/CLIMADA-

668   project/climada_python, last access: 17 July 2019, 2019a.

669 Bresch, D. N., Aznar Siguan, G., Bozzini, V., Bungener, R., Eberenz, S., Hartman, J., Mühlhofer, E., Pérus, M.,

670   Röösli, T., Sauer, I., Schmid, E., Stalhandske, Z., Steinmann C., Stocker, D.: CLIMADA_python v1.4.1

671   http://doi.org/10.5905/ethz-1007-252, 2020.

672 Catto, J. L., Ackerley, D., Booth, J. F., Champion, A. J., Colle, B. A., Pfahl, S., Pinto, J. G., Quinting, J. F., and

673   Seiler, C.: The future of midlatitude cyclones, Curr. Clim. Change Rep., 5, 407-420,

674   https://doi.org/10.1007/s40641-019-00149-4, 2019.

675 Davies, T., Cullen, M. J. P., Malcolm, A. J., Mawson, M. H., Staniforth, A., White, A. A., and Wood, N.: A new

676   dynamical core for the Met Office's global and regional modelling of the atmosphere, Q. J. Roy. Meteor.

677   Soc., 131, 1759-1782, https://doi.org/10.1256/qj.04.101, 2005.

678 Dawkins, L. C., Stephenson, D. B., Lockwood, J. F., and Maisey, P. E.: The 21st century decline in damaging

679   European windstorms, Nat. Hazards Earth Syst. Sci., 16, 1999-2007, https://doi.org/10.5194/nhess-16-

680   1999-2016, 2016.

19

681 Dee, D. P., Uppala, S. M., Simmons, A. J., Berrisford, P., Poli, P., Kobayashi, S., Andrae, U., Balmaseda, M.
682   A., Balsamo, G., Bauer, P., Bechtold, P., Beljaars, A. C. M., van de Berg, L., Bidlot, J., Bormann, N.,
683   Delsol, C., Dragani, R., Fuentes, M., Geer, A. J., Haimberger, L., Healy, S. B., Hersbach, H., Hólm, E. V.,
684   Isaksen, L., Kållberg, P., Köhler, M., Matricardi, M., McNally, A. P., Monge-Sanz, B. M., Morcrette, J.-J.
685   Park, B.-K., Peubey, C., de Rosnay, P., Tavolato, C., Thépaut, J.-N., and Vitart, F.: The ERA-Interim
686   reanalysis: configuration and performance of the data assimilation system, Q. J. Roy. Meteor. Soc., 137,
687   553-597, https://doi.org/10.1002/qj.828, 2011.

688 Della-Marta, P. M., Liniger, M. A., Appenzeller, C., Bresch, D. N., Koellner-Heck, P., and Muccione, V.:
689   Improved estimates of the European winter windstorm climate and the risk of reinsurance loss using
690   climate model data, J. Appl. Meteor. Climatol., 49, 2092-2120, https://doi:10.1175/2010JAMC2133.1,
691   2010.

692 Donat, M. G., Pardowitz, T., Leckebusch, G. C., Ulbrich, U., and Burghoff, O.: High-resolution refinement of a
693   storm loss model and estimation of return periods of loss-intensive storms over Germany, Nat. Hazards
694   Earth Syst. Sci., 11, 2821-2833, https://doi.org/10.5194/nhess-11-2821-2011, 2011.

695 Eberenz, S., Stocker, D., Röösli, T., and Bresch, D. N.: Exposure data for global physical risk assessment, Earth
696   Syst. Sci. Data Discuss., https://doi.org/10.5194/essd-2019-189, in review, 2019.

697 Etienne, C. and Beniston, M.: Wind storm loss estimations in the Canton of Vaud (Western Switzerland), Nat.
698   Hazards Earth Syst. Sci., 12, 3789-3798, https://doi.org/10.5194/nhess-12-3789-2012, 2012.

699 Feuerstein, B., Groenemeijer, P., Dirksen, E., Hubrig, M., Holzer, A. M., and Dotzek, N.: Towards an improved
700   wind speed scale and damage description adapted for Central Europe, Atmospheric Research, 100, 547-
701   564, https://doi.org/10.1016/j.atmosres.2010.12.026, 2011.

702 Geiger, T., Frieler, K., and Bresch, D. N.: A global historical data set of tropical cyclone exposure (TCE-DAT),
703   Earth Syst. Sci. Data, 10, 185–194, https://doi.org/10.5194/essd-10-185-2018, 2018.

704 Gettelman, A., Bresch, D. N., Chen, C. C., Truesdale, J. E., and Bacmeister, J. T.: Projections of future tropical
705   cyclone damage with a high-resolution global climate model, Clim. Change, 146, 575-585,
706   https://doi.org/10.1007/s10584-017-1902-7, 2018.

707 GIN platform: https://www.info.gin.admin.ch/bafu_gin/en/home/gin/overview.html, last access: 19 November
708   2019.

709 GIS browser Zurich: http://web.maps.zh.ch/, last access: 18 September 2019.

710 GNU operating system: GNU General Public License, version 3, https://www.gnu.org/licenses/gpl.html, last
711   access: 17 July 2019, 2007.

712 GVZ annual report: https://www.gvz.ch/_file/1228/01111018003-web-gvz-gb2018-210x297-es-anhang.pdf, last
713   access: 21 February 2020, 2018.

714 GVZ homepage: https://www.gvz.ch/, last access: 14 January 2020.

20

715   Haas, R. and Pinto, J. G.: A combined statistical and dynamical approach for downscaling large-scale footprints
716   of European windstorms, Geophys. Res. Lett., 39, L23804, https://doi.org/10.1029/2012GL054014, 2012.

717   Heneka, P., Hofherr, T., Ruck, B., and Kottmeier, C.: Winter storm risk of residential structures – model
718   development and application to the German state of Baden-Württemberg, Nat. Hazards Earth Syst. Sci., 6,
719   721–733, https://doi:10.5194/nhess-6-721-2006, 2006.

720   Hersbach, H. and Dee, D.: ERA-5 reanalysis is in production, ECMWF Newsletter, Reading, UK, 2016.

721   Imhof, M.: Analyse langfristiger Gebäudeschadendaten, Interkantonaler Rückversicherungsverband IRV, Bern,
722   Switzerland, 2011.

723   IPCC: Climate Change 2014: Impacts, Adaptation and Vulnerability. Part A: Global and Sectoral Aspects.
724   Contribution of Working Group II to the Fifth Assessment Report of the Intergovernmental Panel on
725   Climate Change, edited by: Field, C. B., Barros, V. R., Dokken, D. J., Mach, K. J., Mastrandrea, M. D.,
726   Bilir, T. E.,Chatterjee, M., Ebi, K. L., Estrada, Y. O., Genova, R. C., Girma, B., Kissel, E. S., Levy, A. N.,
727   MacCracken, S., Mastrandrea, P.R., and White, L. L., Cambridge University Press, Cambridge, UK, and
728   New York, USA, 2014.

729   Klawa, M. and Ulbrich, U.: A model for the estimation of storm losses and the identification of severe winter
730   storms in Germany, Nat. Hazard Earth Syst. Sci., 3, 725-732, 2003.

731   Koks, E. and Haer, T.: A high-resolution wind damage model using OpenStreetMap.
732   https://doi.org/10.13140/RG.2.2.23053.59360/2, 2018.

733   Lamb, H. H. and Frydendahl, K.: Historic storms of the North Sea, British Isles, and Northwest Europe,
734   Cambridge University Press, Cambridge, UK, 1991.

735   Leckebusch, G. C., Renggli, D., and Ulbrich, U.: Development and application of an objective storm severity
736   measure for the Northeast Atlantic region, Meteorol. Z., 17, 575-587, 2008.

737   Mitchell-Wallace, K., Jones, M., Hilier, J., and Foote, M.: Natural Catastrophe Risk Management and
738   Modelling: A Practitioners Guide, John Wiley and Sons Ltd, Chichester, UK, 2017.

739   Munich Re: Winter storms in Europe (II): Analysis of 1999 losses and loss potentials, Munich Re, Munich,
740   Germany, 2002.

741   OpenStreetMap contributors: Planet dump retrieved from https://planet.openstreetmap.org,
742   https://www.openstreetmap.org, last access: 25 February 2020, 2017.

743   PERILS: https://www.perils.org/losses?year=1999&classification=&status=#event-losses, last access:
744   31 January 2020.

745   Poli, P., Hersbach, H., Dee, D. P., Berrisford, P., Simmons, A. J., Vitart, F., Laloyaux, P., Tan, D. G. H.,
746   Peubey, C., Thépaut, J.-N., Trémolet, Y., Hólm, E. V., Bonavita, M., Isaksen, L., and Fisher, M.: ERA-
747   20C: An atmospheric reanalysis of the Twentieth Century, J. Climate, 29, 4083–4097,
748   https://doi.org/10.1175/JCLI-D-15-0556.1, 2016.

21

749 Prahl, B. F., Rybski, D., Kropp, J. P., Burghoff, O., and Held, H.: Applying stochastic small-scale damage
750   functions to German winter storms, Geophys. Res. Lett., 39, L06806, https://doi:10.1029/2012GL050961,
751   2012.

752 Prahl, B. F., Rybski, D., Burghoff, O., and Kropp, J. P.: Comparison of storm damage functions and their
753   performance, Nat. Hazards Earth Syst. Sci., 15, 769-788, https://doi.org/10.5194/nhess-15-769-2015, 2015.

754 Raible, C. C., Kleppek, S., Wüest, M., Bresch, D. N., Kitoh, A., Murakami, H., and Stocker, T. F.: Atlantic
755   hurricanes and associated insurance loss potentials in future climate scenarios: limitations of high-
756   resolution AGCM simulations, Tellus, Ser. A Dyn. Meteorol. Oceanogr., 64, 15672,
757   https://dx.doi.org/10.3402/tellusa.v64i0.15672, 2012.

758 Reguero, B. G., Bresch, D. N., Beck, M. W., Calil, J., and Meliane, I.: Coastal risks, nature-based defenses and
759   the economics of adaptation: an application in the Gulf of Mexico, USA; Coast. Eng. Pro. 1, 25,
760   https://dx.doi.org/10.9753/icce.v34.management.25, 2014.

761 Renggli, D. and Zimmerli, P.: Winter storms in Europe: messages from forgotten catastrophes, Swiss Re
762   publication 1507205_16_EN, https://media.swissre.com/documents/Swiss_Re_Winter_storms.pdf, last
763   access: 06 February 2020, 2016.

764 Roberts, J. F., Champion, A. J., Dawkins, L. C., Hodges, K. I., Shaffrey, L. C., Stephenson, D. B., Stringer, M.
765   A., Thornton, H. E., and Youngman, B. D.: The XWS open access catalogue of extreme European
766   windstorms from 1979 to 2012, Nat. Hazards Earth Syst. Sci., 14, 2487–2501,
767   https://doi.org/10.5194/nhess-14-2487-2014, 2014.

768 Röösli, T., Bresch, D.N.: Probabilistic Windstorm Hazard Event Set for Europe, ETH Zurich Research
769   Collection, https://doi.org/10.3929/ethz-b-000406567, 2020.

770 Röösli, T., Bresch, D. N., and Wüest, M.: A comparison of the WISC events sets with both industry and
771   research data, WISC Summary Report of Task 5.3 − ETH / Swiss Re Case Study,
772   https://doi.org/10.3929/ethz-b-000269483, 2018.

773 Schadenstatistik VKG: http://www.vkg.ch/de/versicherung/rueckversicherung, last access: 25 February 2020.

774 Scherrer, S., Salamin, C., Weusthoff, T., Kaufmann, P., Bader, S., Röösli, T., Aemisegger, N., and Gut, M.: Der
775   Wintersturm Burglind/Eleanor in der Schweiz, Fachbericht MeteoSchweiz, 268, 2018.

776 Schwierz, C., Köllner-Heck, P., Zenklusen Mutter, E., Bresch, D. N., Vidale, P.-L., Wild, M., Schär, C.:
777   Modelling European winter wind storm losses in current and future climate, Clim. Change, 101, 485-514,
778   https://doi.org/10.1007/s10584-009-9712-1, 2010.

779 Stucki, P., Brönnimann, S., Martius, O., Welker, C., Imhof, M., von Wattenwyl, N., and Philipp, N.: A catalog
780   of high-impact windstorms in Switzerland since 1859, Nat. Hazards Earth Syst. Sci., 14, 2867-2882,
781   https://doi.org/10.5194/nhess-14-2867-2014, 2014.

782 Stucki, P., Brönnimann, S., Martius, O., Welker, C., Rickli, R., Dierer, S., Bresch, D. N., Compo, G. P., and
783   Sardeshmukh, P. D.: Dynamical downscaling and loss modeling for the reconstruction of historical

22

784 weather extremes and their impacts: A severe foehn storm in 1925, Bull. Am. Meteorol. Soc., 96, 1233-
785 1241, https://doi.org/10.1175/BAMS-D-14-00041.1, 2015.

786 Surminski, S., Westcott, M., Ward, J., Sayers, P., Bresch, D. N., and Bronwyn, C., 2020: Be prepared –
787 exploring future climate-related risk for residential and commercial real-estate portfolios, accepted for
788 publication in 2020 by the Journal of Alternative Investments, 2020.

789 Swisstopo DEM: https://shop.swisstopo.admin.ch/en/products/height_models/dhm25200, last access:
790 8 August 2019.

791 The Economics of Climate Adaptation Working Group: Shaping climate resilient development. A framework
792 for decision-making, joint report by ClimateWorks Foundation, Global Environmental Facility, European
793 Commission, McKinsey & Co., The Rockefeller Foundation, Standard Chartered Banks and SwissRe,
794 https://ethz.ch/content/dam/ethz/special-interest/usys/ied/wcr-
795 dam/documents/Economics_of_Climate_Adaptation_ECA.pdf#page=100, 2009.

796 UPSCALE: http://proj.badc.rl.ac.uk/upscale, last access: 21 February 2020.

797 Walz, M. A. and Leckebusch, G. C.: Loss potentials based on an ensemble forecast: How likely are winter
798 windstorm losses similar to 1990?, Atmos. Sci. Lett., 20, e891, https://doi.org/10.1002/asl.891, 2019.

799 Welker, C. and Martius, O.: Large-scale atmospheric flow conditions and sea surface temperatures associated
800 with hazardous winds in Switzerland, Clim. Dyn., 44, 1857-1869, https://doi.org/10.1007/s00382-014-
801 2404-1, 2015.

802 Welker, C., Martius, O., Stucki, P., Bresch, D. N., Dierer, S., and Brönnimann, S.: Modelling economic losses
803 of historic and present-day high-impact winter windstorms in Switzerland, Tellus, Ser. A Dyn. Meteorol.
804 Oceanogr., 68, 29546, doi:10.3402/tellusa.v68.29546, 2016.

805 WISC products: https://wisc.climate.copernicus.eu/wisc/#/help/products, last access: 26 July 2019.

806 WISC hazard event set description:
807 https://wisc.climate.copernicus.eu/wisc/documents/shared/C3S_WISC_Event%20Set_Description_v1.0.pd
808 f, last access: 26 July 2019.

809 World Bank: Building the World Bank's Wealth Accounts: Methods and Data, Environment and Natural
810 Resources Global Practice, World Bank, https://development-data-hub-s3-
811 public.s3.amazonaws.com/ddhfiles/94641/wealth-methodology-january-30-2018_4_0.pdf, last access:
812 14 January 2019, 2018.

813 Zurich construction price index: https://www.stadt-zuerich.ch/prd/de/index/statistik/themen/bauen-
814 wohnen/wohnbaupreise/zuercher-index-der-wohnbaupreise.html, last access: 14 January 2020.

23

815 **Table 1:** Summary statistics for the windstorm hazard event sets and insurance claims data used in this study.

Dataset	Available years (period)	Total number of available windstorm hazard events	Number of damage events in the canton of Zurich
"WISC historic"	75 (1940-2014)	142	27
"WISC probabilistic extension"	2'250 (30*75)	142 (parent events) and 4'118 (altered offspring events)	754
"WISC synthetic"	405 (3*135)	22'980	42
"WISC operational"	39 (1979-2017)	106	untested
"Observed footprints"	2 (2017-2018)	7	7
Insurance claims data	36 (1981-2014 and 2017-2018)	-	18 ("WISC historic") and 7 ("observed footprints")

816 **Table 2:** Annual average damage (AAD) and event damage for different return periods (RP) and the windstorm
817 event Lothar/Martin on the basis of insurance claims data and modelled damages using the GVZ damage model
818 and the hazard event sets "WISC historic" and "WISC probabilistic extension", respectively.

	Available years (period)	AAD [CHF m.]	Event damage with 5-year RP [CHF m.]	Event damage with 10-year RP [CHF m.]	Event damage with 50-year RP [CHF m.]	Event damage with 250-year RP [CHF m.]	Event damage due to Lothar/ Martin [CHF m.]
Insurance claims data	34 (1981-2014)	2.3	0.6	1.1	-	-	62.4
"WISC historic"	75 (1940-2014)	1.4	0.2	1.3	31.4	-	62.7
"WISC probabilistic extension"	2'250 (30*75)	1.4	0.2	1.3	17.0	74.6	-

819

24
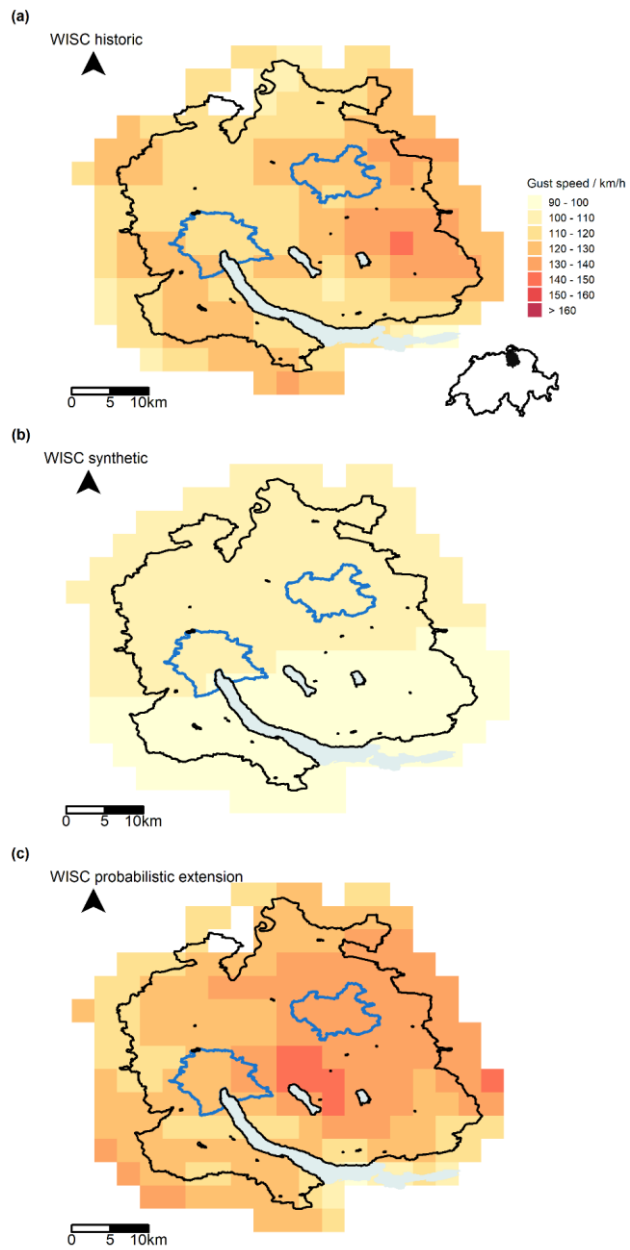
Figure 1: Maximum wind gusts for every grid cell in the canton of Zurich (i.e., windstorm footprints) for the most damaging events in **(a)** "WISC historic", **(b)** "WISC synthetic", and **(c)** "WISC probabilistic extension". The urban areas of the two main cities Zurich (left) and Winterthur (right) are marked in blue.
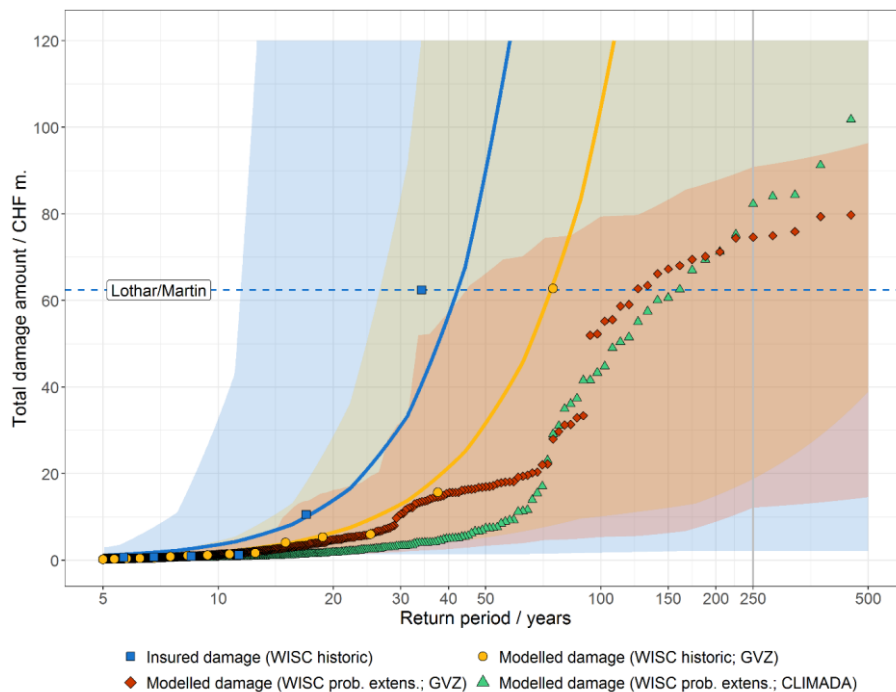
824

825
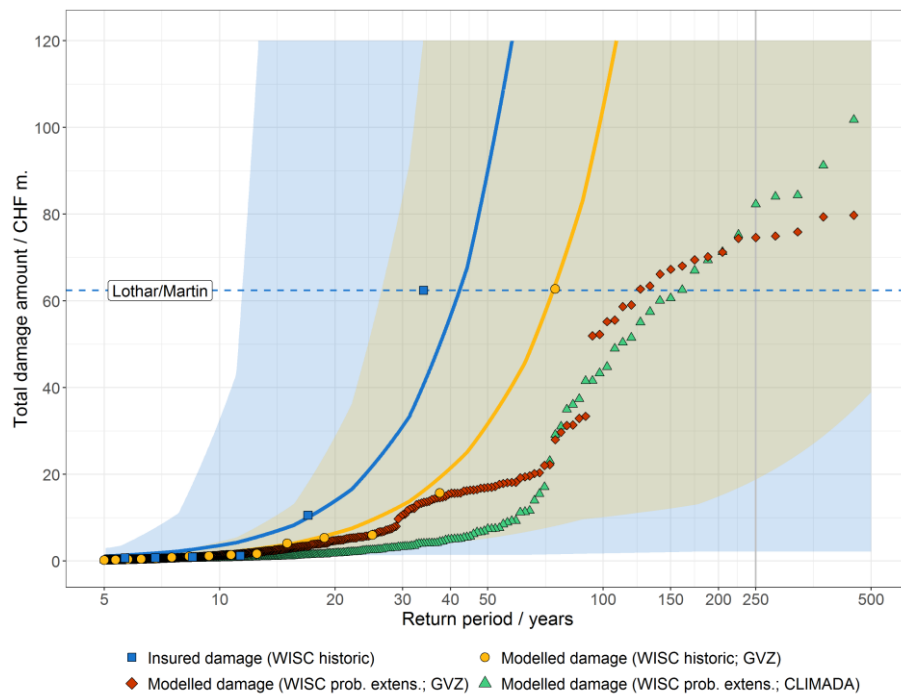
Figure 2: Exceedance frequency curves for building damages in the canton of Zurich based on different data sources. The blue squares indicate the insured damages according to GVZ's database (excluding the additional windstorms in 2017 and 2018), the blue solid line represents a GPD fitted to the insured damages, and the blue ribbon is the 90-% confidence interval produced by resampling. The yellow dots, solid line, and ribbon are analogous to the blue, but for the modelled damages based on "WISC historic" and the GVZ damage model. The red diamonds (green triangles) show the exceedance frequency curve of the modelled damages based on the hazard event set "WISC probabilistic extension" and the GVZ damage model (CLIMADA). The red ribbon shows the probabilistic envelope for the modelled damages based on "WISC probabilistic extension" and the GVZ damage model computed by applying a bootstrapping approach as described in Sect. 2.4.3. The insured total damage for Lothar/Martin is shown by a blue dashed horizontal line, and the 250-year return period is indicated by a grey solid vertical line.

27
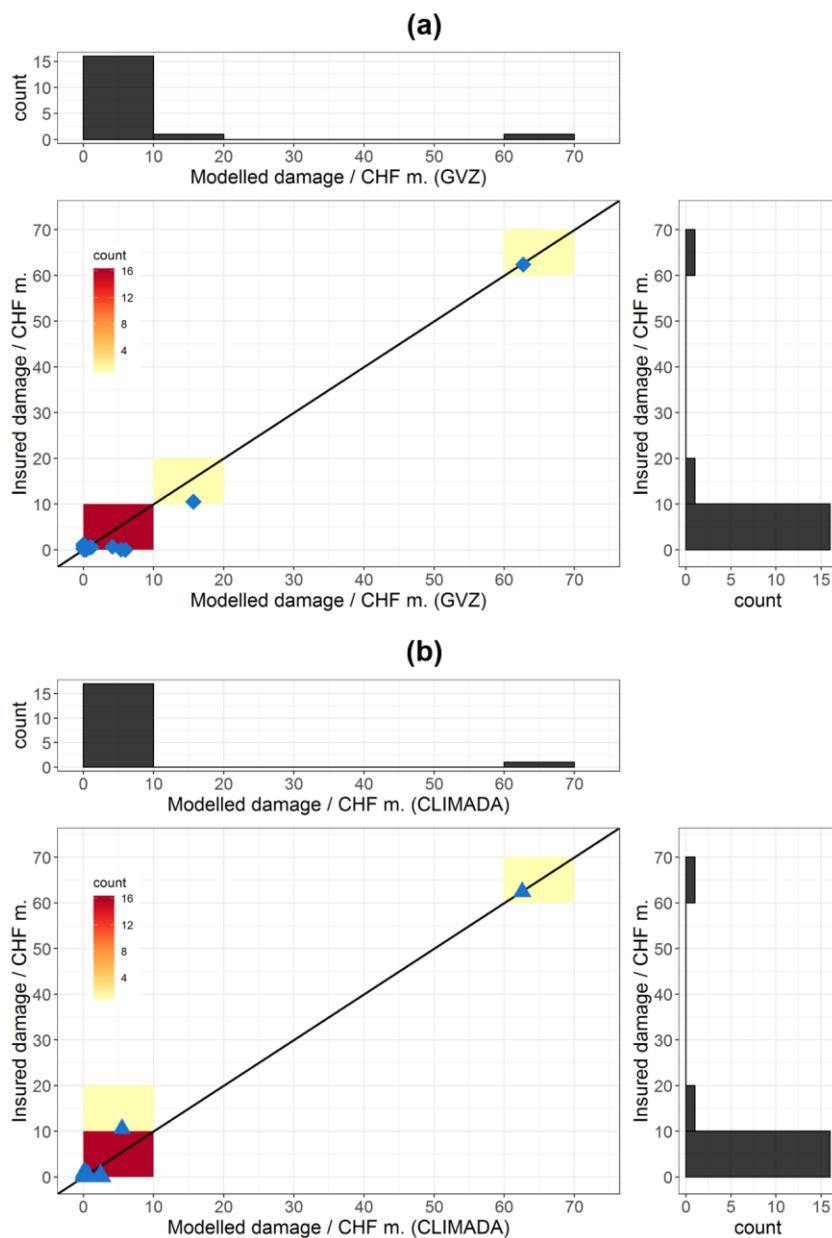
Figure 3: 2d-histograms for the normalised insured total damages in the canton of Zurich versus the modelled total damages based on **(a)** the GVZ damage model (diamonds) and **(b)** the CLIMADA impact model (triangles), respectively, for all windstorms with damage > 0 in the hazard event set "WISC historic". Marginal histograms are shown in the top and right panels.

28
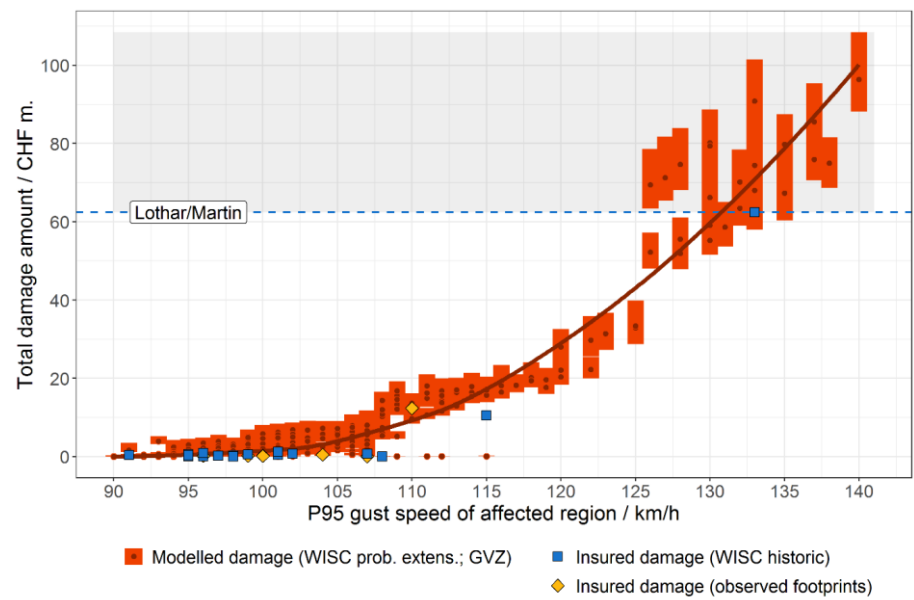
Figure 4: Total damage modelled using the GVZ damage model and the hazard event set "WISC probabilistic extension" versus the 95th percentile of the corresponding gust speeds in the affected region of the canton of Zurich (median of 1'000 random damage modelling as red points; range of modelled damages indicated as red bars). The 95th percentile of the gust speeds is shown, because the 95th percentile is used in GVZ's damage model to categorise windstorm events (Sect. 2.3.1). The relationship between wind gust speed and modelled total damage is further approximated by a locally estimated scatterplot smoothing (LOESS) and a bootstrap method (i.e., random resampling with replacement, number of samples = 1'000; median of confidence interval given as solid red line). Furthermore, the relationship between gust speeds and normalised insured total damages based on "WISC historic" and independent, interpolated wind gust observations (selection of windstorms in 2017 and 2018, including winter windstorm Burglind) are given as blue squares and yellow diamonds, respectively. The domain for unprecedented windstorm damages − i.e. beyond Lothar/Martin − is shaded grey.

Appendix

857 **Table A1:** AAD and event damage for different return periods (RP) and the windstorm event Lothar/Martin on
858 the basis of insurance claims data and modelled damages using the CLIMADA impact model and the hazard
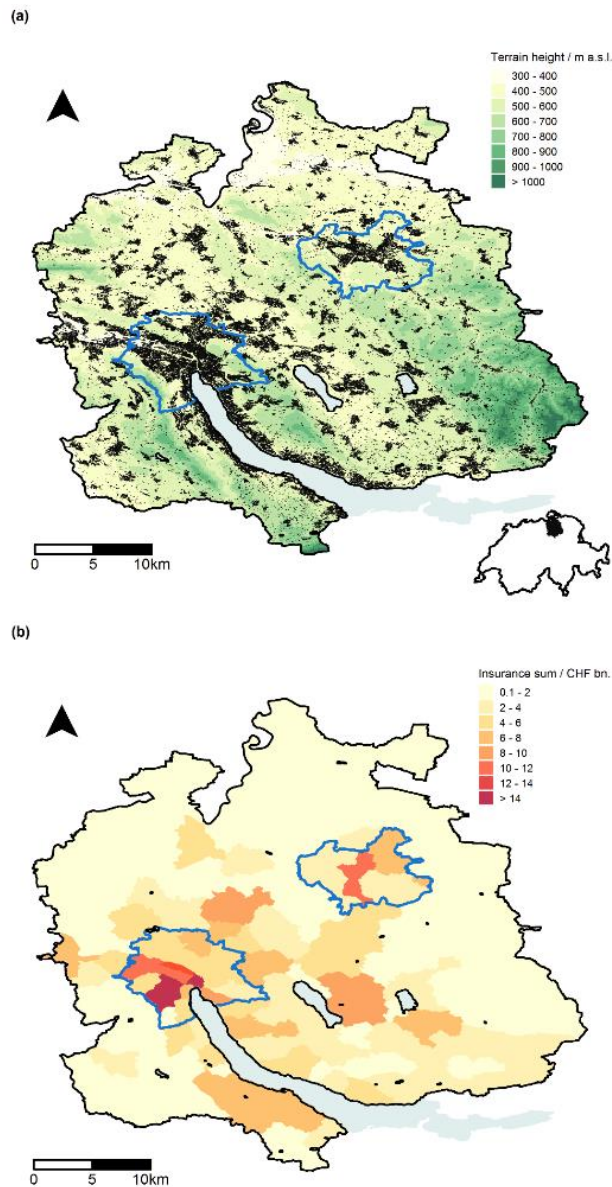859 event sets "WISC historic" and "WISC probabilistic extension", respectively.

|	Available years (period)	AAD [CHF m.]	Event damage with 5-year RP [CHF m.]	Event damage with 10-year RP [CHF m.]	Event damage with 50-year RP [CHF m.]	Event damage with 250-year RP [CHF m.]	Event damage due to Lothar/ Martin [CHF m.]
Insurance claims data	34 (1981-2014)	2.3	0.6	1.1	-	-	62.4
"WISC historic"	75 (1940-2014)	1.1	0.2	0.6	24.5	-	62.6
"WISC probabilistic extension"	2'250 (30*75)	1.2	0.2	0.6	7.4	82.3	-

860

861
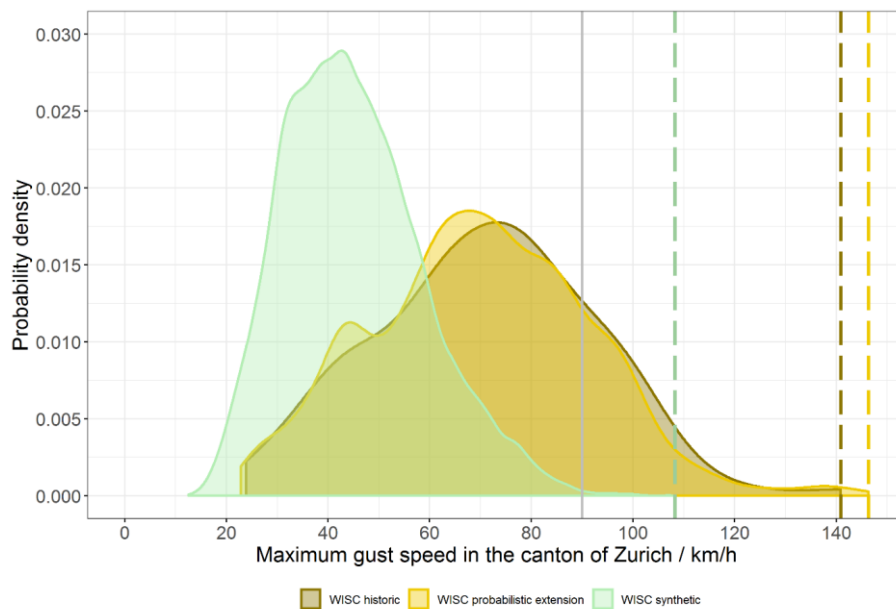
Figure A1: Probability density functions of the maximum gust speeds at building level in the canton of Zurich for the three hazard event sets "WISC historic" (brown), "WISC probabilistic extension" excluding the parent windstorms (yellow), and "WISC synthetic" (green). The maxima of the individual distributions are shown as dashed vertical lines. In the GVZ damage model, damage is possible from a wind gust speed of more than 90 km/h, which is here indicated by a grey solid vertical line.

(a)

Terrain height / m a.s.l.
- 300 - 400
- 400 - 500
- 500 - 600
- 600 - 700
- 700 - 800
- 800 - 900
- 900 - 1000
- > 1000

0 5 10km

(b)

Insurance sum / CHF bn.
- 0.1 - 2
- 2 - 4
- 4 - 6
- 6 - 8
- 8 - 10
- 10 - 12
- 12 - 14
- > 14

0 5 10km

867

Figure A2: (a) Terrain height for the canton of Zurich (colour scheme) according to a digital elevation model with a horizontal grid size of 200 m (source: Swiss Federal Office of Topography; Swisstopo DEM, 2019). In addition, the spatial distribution of all buildings insured by GVZ is indicated and the urban areas of the two main cities, Zurich (left) and Winterthur (right), are marked in blue. **(b)** Total building sum insured for each municipality (colour scheme).
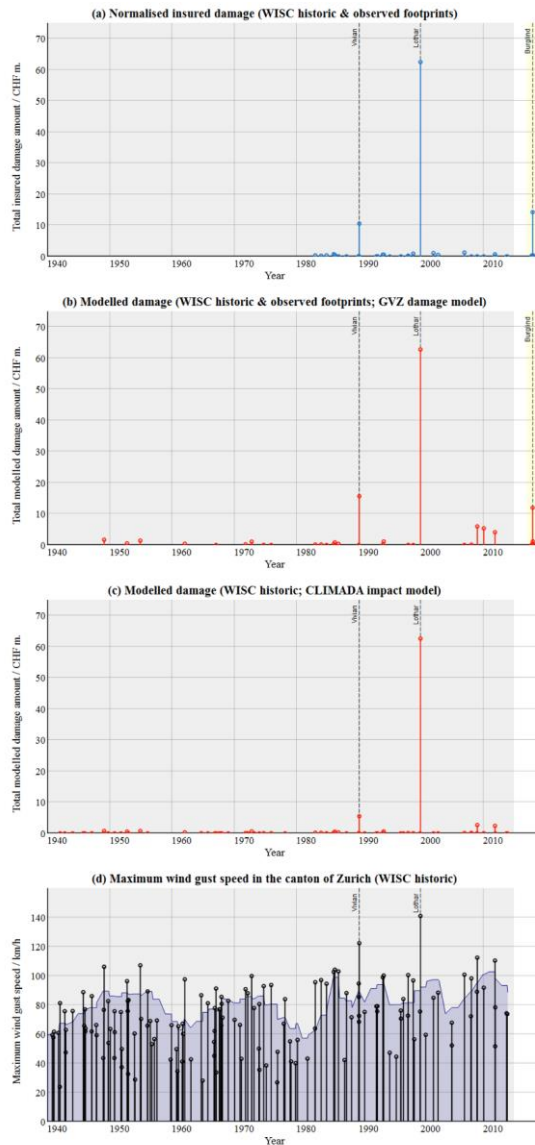
Figure A3: Variability of windstorms and associated damages in the canton of Zurich: **(a)** normalised insured damage, **(b)** modelled windstorm damage based on the GVZ damage model and the hazard event sets "WISC historic" and "observed footprints", **(c)** modelled windstorm damage based on the CLIMADA impact model and "WISC historic", and **(d)** maximum gust speeds at building level in the canton of Zurich according to "WISC historic" (black stem plot). The filled time series in (d) additionally shows the 5-year moving average of the yearly maximum gust speeds in the canton of Zurich. The period for which "WISC historic" hazard data ("observed footprints") is available is shaded grey (yellow) in (a) and (b). The windstorm events Vivian/Wiebke, Lothar/Martin, and Burglind are marked.

33